UNIVERSITY OF COPENHAGEN

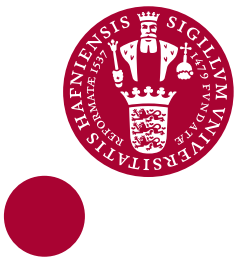

Srs2 promotes Mus81-Mms4-mediated resolution of recombination intermediates

Chavdarova, Melita; Marini, Victoria; Sisakova, Alexandra; Sedlackova, Hana; Vigasova, Dana; Brill, Steven J.; Lisby, Michael; Krejci, Lumir

Published in:
Nucleic Acids Research

DOI:
10.1093/nar/gkv198

Publication date:
2015

Document version
Publisher's PDF, also known as Version of record

Document license:
CC BY

Citation for published version (APA):
Chavdarova, M., Marini, V., Sisakova, A., Sedlackova, H., Vigasova, D., Brill, S. J., Lisby, M., & Krejci, L. (2015). Srs2 promotes Mus81-Mms4-mediated resolution of recombination intermediates. *Nucleic Acids Research*, *43*(7), 3626-3642. https://doi.org/10.1093/nar/gkv198

Download date: 05. maj. 2023

3626–3642 *Nucleic Acids Research, 2015, Vol. 43, No. 7* *Published online 12 March 2015*
doi: 10.1093/nar/gkv198

Srs2 promotes Mus81–Mms4-mediated resolution of recombination intermediates

Melita Chavdarova[1,2], Victoria Marini[1], Alexandra Sisakova[1,3], Hana Sedlackova[1], Dana Vigasova[1,4], Steven J. Brill[5], Michael Lisby[6] and Lumir Krejci[1,2,3,*]

[1]Department of Biology, Masaryk University, Kamenice 5/A7, Brno 625 00, Czech Republic, [2]National Centre for Biomolecular Research, Masaryk University, Kamenice 5/A4, Brno 625 00, Czech Republic, [3]International Clinical Research Center, Center for Biomolecular and Cellular Engineering, St. Anne's University Hospital Brno, Brno, Czech Republic, [4]Department of Genetics, Cancer Research Institute, Vlarska 7, 833 91 Bratislava, Slovakia, [5]Department of Molecular Biology and Biochemistry, Rutgers University, Piscataway, NJ, USA and [6]Department of Biology, University of Copenhagen, Ole Maaløes Vej 5, DK-2200 Copenhagen N, Denmark

Received August 06, 2014; Revised February 13, 2015; Accepted February 26, 2015

Downloaded from http://nar.oxfordjournals.org/ at Danmarks NaturOG on May 2, 2016

ABSTRACT

A variety of DNA lesions, secondary DNA structures or topological stress within the DNA template may lead to stalling of the replication fork. Recovery of such forks is essential for the maintenance of genomic stability. The structure-specific endonuclease Mus81–Mms4 has been implicated in processing DNA intermediates that arise from collapsed forks and homologous recombination. According to previous genetic studies, the Srs2 helicase may play a role in the repair of double-strand breaks and ssDNA gaps together with Mus81–Mms4. In this study, we show that the Srs2 and Mus81–Mms4 proteins physically interact *in vitro* and *in vivo* and we map the interaction domains within the Srs2 and Mus81 proteins. Further, we show that Srs2 plays a dual role in the stimulation of the Mus81–Mms4 nuclease activity on a variety of DNA substrates. First, Srs2 directly stimulates Mus81–Mms4 nuclease activity independent of its helicase activity. Second, Srs2 removes Rad51 from DNA to allow access of Mus81–Mms4 to cleave DNA. Concomitantly, Mus81–Mms4 inhibits the helicase activity of Srs2. Taken together, our data point to a coordinated role of Mus81–Mms4 and Srs2 in processing of recombination as well as replication intermediates.

INTRODUCTION

Homologous recombination (HR) is responsible for the repair of DNA double-strand breaks (DSBs), single-stranded DNA gaps, shortened telomeres and stalled or collapsed replication forks. HR repair is characterized by the assembly of the Rad51 protein on single-stranded DNA to form the so-called presynaptic filament. These nucleoprotein filaments search for homology and mediate the invasion of the sister chromatid resulting in the formation of joint DNA molecules called D-loops (1,2). After D-loop formation, repair can proceed by two alternative pathways. In classical double-strand break repair (DSBR), the D-loop is stabilized by capture of the second end of the DSB which leads to the generation of a double-Holliday Junction (dHJ). In the alternative pathway, synthesis-dependent strand-annealing (SDSA), the invading strand is extended by DNA polymerase but then displaced from the D-loop and annealing with the second end of the DSB (Figure 8 (2,3)).

Numerous proteins have been implicated in HR. Among them, the Srs2 protein stands out with its multiple roles during this process (4). It is a 3′–5′ DNA helicase (5,6) related to the bacterial UvrD protein (7). Apart from the ability to dismantle Rad51 filament and thereby inhibit HR (8,9), Srs2 appears to promote the SDSA pathway (10,11) by facilitating displacement of Rad51 from non-invading ssDNA end or by regulating elongation of the invading strand during HR to prevent second-end capture (12). Srs2 is also directly involved in both branches of post replication repair (PRR), where it could play an important role in the decision between error-free or error-prone pathways (13–15). It is also required for proper checkpoint activation, as well as recovery and adaptation in response to cell cycle arrest (16,17). Many synthetic-lethal interactions with Srs2 result in accumulation of toxic recombination intermediates (18–21).

Mus81 has been implicated in processing various replication and recombination intermediates. It is a structure-selective endonuclease that shares homology with the XPF/Rad1 family of proteins. Members of this family usually form a heterodimeric complex with partner proteins (22). While the *Saccharomyces cerevisiae* partner protein for Mus81 has been identified as Mms4, in fission yeast and mammalian cells, Eme1 forms a complex with

*To whom correspondence should be addressed. Tel: +420 549493767; Fax: +420 549492556; Email: lkrejci@chemi.muni.cz

© The Author(s) 2015. Published by Oxford University Press on behalf of Nucleic Acids Research.
This is an Open Access article distributed under the terms of the Creative Commons Attribution License (http://creativecommons.org/licenses/by-nc/4.0/), which permits non-commercial re-use, distribution, and reproduction in any medium, provided the original work is properly cited. For commercial re-use, please contact journals.permissions@oup.com

Mus81 with similar activities to those of its budding yeast counterpart (23,24). Biochemical studies have demonstrated that Mus81–Mms4 has preferences for a number of DNA structures, such as nicked HJs, D-loops, 3′-flaps and forks (24–27). However, it still remains unclear whether Holliday junctions (HJs), the central intermediates in the HR process, are direct physiological substrates for the Mus81–Mms4 (Eme1) complex (25,27–28). In addition, *mus81/mms4/eme1* mutants are hypersensitive to a range of agents including methyl methanesulfonate (MMS), camptothecin (CPT), hydroxyurea (HU) and UV light, suggesting a role for this complex in processing aberrant DNA junctions formed at stalled replication forks (29–32). Both budding and fission yeast *mus81/mms4/eme1* mutants reduce or eliminate meiotic recombination indicating a role in processing intermediates during meiosis (32,33). Similarly to Srs2, deletion of Mus81 was shown to be synthetically lethal with mutation in *SGS1* and this lethality can be suppressed by elimination of HR (18,32,34).

In this study, we show that the *S. cerevisiae* proteins, Srs2 and Mus81–Mms4 directly associate *in vitro* and frequently co-localize *in vivo*. We mapped the interaction domains within the Srs2 and Mus81 proteins and found that the interaction leads to a dramatic stimulation of Mus81–Mms4 nuclease activity. This stimulation is independent of the Srs2's helicase/ATPase activity and its SUMO/PCNA interaction domain. In addition, Srs2 relieves the inhibition of Mus81–Mms4 nuclease activity by Rad51, but in an ATPase-dependent manner. At the cellular level, the functional interaction between Srs2 and Mus81 is supported by their co-localization at damage-induced foci. Taken together, the stimulation of Mus81–Mms4 nuclease activity by Srs2 might be required not only for processing classical recombination intermediates but also for the rescue of arrested forks.

MATERIALS AND METHODS

Yeast strains and plasmids

Standard procedures for yeast mating, sporulation, dissection, transformation and preparation of growth media (35,36) were used to obtain strains for this study (Supplementary Table S1). All yeast strains used are derivatives of W1588–4C (*MAT***a** *ade2–1 can1–100 ura3–1 his3–11, 15 leu2–3,112 trp1–1*) (37) a *RAD5* derivative of W303–1A (38).

Plasmids used in this study are described in Supplementary Table S2. Oligonucleotides used for construction are listed in Supplementary Table S3. The Srs2$^{783–1174}$::pGEX-6P-1 fragment was amplified by PCR and cloned into the *Eco*RI site of pGEX-6P-1.Srs2$^{783–998}$::pGEX-6P-1 and Srs2$^{783–898}$::pGEX-6P-1 were created by site-directed mutagenesis of Srs2$^{783–1174}$::pGEX-6P-1 by producing stop codons at corresponding positions. Fragment Srs2$^{898–998}$ was amplified by polymerase chain reaction (PCR) and cloned into the *Eco*RI site of pGEX-6P-1. Construction of Srs2$^{998–1174}$ fragment in pGEX-6P-1 was described earlier (12). The N-terminal truncation of Srs2 $^{1–700}$::pET11c was made by site-directed mutagenesis of Srs2::pET11c by adding stop codon at corresponding positions. Plasmid pKR6317 was constructed by amplifying the first 319aa of Mus81 on an *Nde*I-*Not*I PCR fragment using oligos 462 (GAACATATGGAACTCTCATCAAACTTA) and 924 (TTTGCGGCCGCCTACTGTTTGATCATCA GA) and ligating it together with an 88-bp *Not*I-*Bam*HI linker into the *Nde*I-*Bam*HI sites of pET11a. This construct expresses amino acids 1–319 of Mus81 fused to a 26aa C-terminal V5-His6 epitope tag. The Mus81$^{1–319}$ fragment was cloned as a *Nde*I/*Bam*HI fragment from Mus81$^{1–319}$::pET11a into the pGBKT7 yeast two-hybrid vector. Plasmids containing Mus81$^{1–245}$, Mus81$^{1–220}$ and Mus81$^{1–155}$ fragments in two-hybrid vectors were generated by site-directed mutagenesis to incorporate appropriate stop codons. The plasmid for GAL inducible expression of Mre11 protein contains the Mre11 open reading frame (ORF) amplified by PCR and cloned into *Bam*HI site of pPM271 vector.

Expression and purification of Srs2 and its variants

Wild-type Srs2, Srs2-K41R and Srs2$^{1–860}$ were expressed and purified as previously described (39,40). Another N-terminal truncation of Srs2 (Srs2$^{1–898}$) was purified as described (41). Srs2$^{1–700}$ was expressed in Arctic RIL cells and purified the same way as previously described for wild-type Srs2. The C-terminal truncations of Srs2 corresponding to Srs2$^{783–1174}$, Srs2$^{783–998}$, Srs2$^{783–898}$, Srs2$^{898–998}$ and Srs2$^{998–1174}$ were cloned in the pGEX-6P-1 vector and expressed in *Escherichia coli* BL21(DE3) cells by induction with 0.1 mM isopropyl-1-thio-β-D-galactopyranoside (IPTG) overnight at 16°C. After harvesting cells by centrifugation, the cell pellets were resuspended and sonicated in cell-breakage buffer (CBB) (50 mM Tris pH 7.5, 10% sucrose, 10 mM EDTA, 1 mM DTT and 0.01% NP40) containing 150 mM KCl and protease inhibitors (2 μg/ml aprotinin, 5 μg/ml benzamidine, 10 μM chymostatin, 10 μM leupeptin and 1 μM pepstatin A). The crude extract was clarified by ultracentrifugation (100 000 x g, 4°C, 1 h) and the supernatant loaded on SP-Sepharose (7 ml, GE Healthcare). The column was eluted with 70 ml of 150–1000 mM KCl in buffer K (20 mM K_2HPO_4, 10% glycerol, 0.5 mM EDTA). Fractions containing Srs2 were mixed for 1 h at 4°C with 500 μl of GSH-Sepharose (GE Healthcare) and washed in buffer K containing 100 mM KCl. Bound proteins were washed with 5 ml of 100 mM KCl in buffer K and eluted in steps with 500 μl of 10, 50, 100 and 200 mM glutathione (GSH) in buffer K containing 100 mM KCl. The peak fractions, eluting in the range of 20–100 mM GSH, were loaded onto a 1 ml MonoS column (GE Healthcare) and eluted with a 10 ml gradient from 150 to 1000 mM KCl in buffer K. Fragments of Srs2 were concentrated and stored in 5 μl aliquots at −80°C.

Purification of yeast and human Mus81 protein and its complexes

Yeast Mus81–Mms4 and Mus81 proteins as well as human MUS81–EME1 complex were expressed in *E. coli* and purified as previously described (42). For expression of Mus81$^{1–319}$, 10 g of *E. coli* cell paste was sonicated in 50 ml CBB buffer containing 150 mM KCl and clarified as described above. The supernatant was passed through Q-Sepharose (7 ml) and the flow-through fraction was then

Downloaded from http://nar.oxfordjournals.org/ at Danmarks NaturOG on May 2, 2016

directly applied to SP-Sepharose (7 ml) and eluted with a 70 ml gradient of 150–1000 mM KCl in buffer K. Fractions containing Mus81$^{1–319}$ were then mixed with His-Select Ni affinity gel (Qiagen) for 1 h at 4°C. The bound protein was eluted in steps with 500 μl each of 150, 300 and 500 mM imidazole in buffer K containing 150 mM KCl. The peak fraction was loaded on a 1 ml MonoS column (GE Healthcare) and eluted with a 10 ml gradient of 150–1000 mM KCl in buffer K. Nearly homogenous Mus81$^{1–319}$ was concentrated and stored in 5 μl aliquots at −80°C.

Expression and purification of other proteins

The Rad1–Rad10 complex was expressed in *E. coli* strain Rosetta(DE3)pLysS from a bicistronic plasmid containing both 6xHis-Rad1 and Rad10 (32). The overexpression was induced at OD_{600} ∼ 0.8 by addition of 0.1 mM IPTG followed by an incubation at 16°C overnight. The cells were pelleted and stored at −80°C. Extract from 9 g of cell paste was prepared by sonication in 40 ml of CBB buffer. The lysate was clarified by ultracentrifugation (100 000 x g, 4°C, 1 h) and the supernatant was incubated with 1 ml of HIS-Select nickel affinity gel (Sigma) for 1 h at 4°C. The beads were washed with 12 ml of buffer K containing 150 mM KCl. The bound proteins were eluted with buffer K supplemented with 50 mM KCl and containing 50, 150, 300, 500 or 1000 mM imidazole. The fractions containing Rad1–Rad10 complex (from 150 to 500 mM imidazole) were pooled and applied onto a 1 ml Heparin column followed by elution using an 8 ml gradient of 275–1000 mM KCl in buffer K. The peak fractions of Rad1–Rad10 complex eluting from the Heparin column at ∼500 mM KCl were pooled, loaded onto a 0.5 ml MonoQ column and eluted using a 5 ml gradient of 275–1000 mM KCl in buffer K. The fractions containing eluted Rad1–Rad10 complex were concentrated to 400 μl in a VivaSpin-2 concentrator, and then fractionated in a 23 ml Sephacryl S400 column in K buffer containing 300 mM KCl. The peak fractions of Rad1–Rad10 complex were concentrated to 2 μg/μl and stored in small aliquots at −80°C.

The expression of Mre11 was described previously (43). Briefly, overnight cultures grown at 30°C incomplete synthetic media lacking uracil were diluted 8-fold into fresh medium containing galactose and incubated at 30°C for 24 h to induce the expression of Mre11. After harvesting, the cells were lysed with cryo-mill (LABTECH) and yeast powder was resuspended in 100 ml of CBB buffer containing 100 mM KCl and subjected to ammonium sulfate precipitation at 0.28 g/ml. The precipitate was dissolved in 100 ml of buffer K with protease inhibitors and passed through Q-Sepharose (20 ml). Mre11 was eluted with a 200 ml gradient of 100–1000 mM KCl in K buffer and then loaded onto a 1 ml hydroxyapatite column and eluted with a 10 ml gradient of 0–400 mM KH_2PO_4 in buffer K. Fractions containing Mre11 were loaded on a 1 ml MonoS and eluted with a 10 ml gradient of 100–1000 mM KCl in buffer K. The peak fractions containing Mre11 were concentrated and stored at −80°C.

Yeast Rad51 was expressed and purified as described elsewhere (6).

DNA substrates

Oligonucleotides were purchased from VBC Biotech. Sequences of oligonucleotides used for synthetic substrates are shown in Supplementary Table S4. The individual substrates were prepared by annealing of corresponding oligonucleotides as previously described (41).

Nuclease assay

Nuclease assays with Mus81–Mms4 were performed as previously described (42). Briefly, Mus81–Mms4 (0.25 nM) was pre-incubated with Srs2, Srs2-K41R or various truncation proteins (5, 10, 20, 40 and 80 nM) at 30°C for 30 min in 20 μl of buffer N (20 mM Tris, pH 8.0, 100 mM NaCl, 100 μg/ml bovine serum albumin, 0.2 mM dithiothreitol, 5% glycerol and 10 mM $MgCl_2$). DNA (7 nM) was added to the reaction mixtures and incubated for another 30 min at 37°C. After deproteinization by incubation with 0.1% SDS and 500 μg/ml of proteinase K at 37°C for 5 min, reactions were resolved on 10% polyacrylamide gels and scanned with a Fuji FLA 9000 imager (Fuji). In some cases the products were also analyzed on 13% denaturing gel. The experiments were done in triplicates and the gels were quantified by Multi Gauge V3.2 software (Fuji).

In the time course experiment, the indicated amount of Mus81–Mms4 was incubated with 10 nM of Srs2 for 30 min. After addition of fluorescently labeled DNA (7 nM), reaction mixtures were incubated for 10, 20, 30, 40 and 50 min and analyzed as described above. In the targeting assay, Srs2 (70 nM) was first pre-incubated with the 3′-flap structure (6 nM) at 30°C for 10 min followed by addition of Mus81–Mms4 (0.25 nM) and incubation for 2.5, 5, 7.5, 10 and 15 min at 30°C. Corresponding aliquots were analyzed on a 10% native gel as described above. In the reaction containing human MUS81–EME1 protein, Srs2 (10, 20 and 40 nM) was mixed with 0.25 nM MUS81–EME1 and the reaction was performed as described above. For the Rad1–Rad10 reaction, 0.2 nM of Rad1–Rad10 was mixed with 10, 20, 40, 80, 150 and 300 nM Srs2$^{783–898}$ together with Y form DNA substrate (7 nM) and the reaction was carried out as described above.

Rad51 removal assay

In the nuclease assay containing Rad51, increasing concentrations of Rad51 (100, 200, 400, 600 and 800 nM) were pre-incubated with DNA (7 nM) in 20 μl of buffer N and 800 nM ATP for 10 min at 37°C, then Mus81–Mms4 (0.4 nM) was added to the mixture and the reaction was carried out as above. Next, yeast Rad51 (600 nM) was pre-incubated with DNA (7 nM) for 10 min at 37°C followed by addition of Mus81–Mms4 (0.4 nM) together with increasing concentrations of Srs2 or Srs2-K41R mutant (5, 7.5, 10, 15 and 20 nM) and incubated for 30 min at 37°C. After deproteinization, the reactions were resolved on 10% native PAGE and scanned with a Fuji FLA 9000 imager and analyzed.

Pull-down assays

To analyze the interaction between Mus81–Mms4 and Srs2, yeast Mus81–Mms4 complex, Mus81 or Mus81$^{1–319}$ (5

Downloaded from http://nar.oxfordjournals.org/ at Danmarks NaturOG on May 2, 2016

μg each) were pre-incubated with 5 μg of various GST-tagged Srs2 fragments ($Srs2^{783–1174}$, $Srs2^{783–998}$, $Srs2^{783–898}$, $Srs2^{898–998}$ or $Srs2^{998–1174}$) for 1 h at 4°C. After pre-incubation, 10 μl of GSH-Sepharose 4 Fast Flow (GE Healthcare) in 25 μl of buffer K containing 150 mM KCl was added and reactions were incubated for an additional 30 min at 4°C. Supernatants were collected and beads were washed three times with 100 μl of the same buffer. The supernatant and beads were treated with Laemmli buffer and analyzed by sodium dodecyl sulphate-polyacrylamide gel electrophoresis (SDS-PAGE) on a 10% gel followed by Coomassie blue staining or western blot analysis with appropriate antibodies. For the pull-down using the V5 epitope, the same concentrations of Srs2 as well as $Srs2^{1–700}$, $Srs2^{1–898}$ or $Srs2^{1–860}$ were pre-incubated for 1 h at 4°C with Mus81 or $Mus81^{1–319}$. Anti-V5 agarose beads (10 μl in 25 μl of buffer K containing 200 mM KCl) were added and reactions were incubated for 30 min at 4°C. After incubation, the mixtures were treated as described above. Samples were also analyzed by western blot with antibodies against the His affinity tag present at the N-terminus of each Srs2 fragments.

The IP was performed as follows: the plasmid carrying *MUS81* gene was expressed in yeast and grown in YPD at 30°C overnight to $OD_{600} \sim 1$. The frozen pellet was lysed with Immunoprecipitation (IP) buffer (50 mM Tris-HCl pH 7.4, 150 mM NaCl, 0.5% Triton X-100, 1 mM PMSF, 5 μg/μl leupeptin and 1 μg/μl aprotinin) and yeast extract containing wtMus81 was incubated with purified $Srs2^{783–998}$ and 10 μl of Glutathione Sepharose 4 Fast Flow beads for 3 h at 4°C. After incubation, supernatants and beads were analyzed by western blot with anti-His antibodies.

Yeast two-hybrid analysis

Two-hybrid analysis was performed as described previously (44). Yeast strains PJ69–4a carrying pGADT7-$Srs2^{783–1174}$ and PJ69–4α carrying various truncations of Mus81 ($Mus81^{1–155}$, $Mus81^{1–220}$, $Mus81^{1–245}$, $Mus81^{1–288}$, $Mus81^{138–632}$ and $Mus81^{290–632}$) cloned into pGBKT7 (Supplementary Table S2) were mated overnight on a YPD plate to form diploids. Thereafter, the diploid strains were selected on media lacking leucine and tryptophan and grown for 48 h at 30°C. Cells were spotted as 10-fold serial dilutions on medium lacking leucine and tryptophan or leucine, tryptophan and histidine and a picture was taken 3 days after incubation at 30°C. The empty vector (pGADT7) was included as negative control.

Helicase assays

The helicase assays with Srs2 were performed as previously described by Marini 2012 (41). Reaction mixtures containing Srs2 (10 nM) were pre-incubated with increasing concentrations of Mus81–Mms4 (12.5, 25, 50, 100, 200 and 300 nM), Mus81 (12.5, 25, 50 and 100 nM) or $Mus81^{1–319}$ (12.5, 25, 50 and 100 nM) in buffer H (30 mM Tris pH 7.5, 1 mM DTT, 0.1 mg/ml BSA, 100 mM KCl, 20 mM creatine phosphate, 20 μg/ml creatine kinase, 2.4 mM $MgCl_2$ and 2 mM ATP) for 10 min on ice. The reactions with Mre11 included 12.5, 25, 50, 100, 200, 300 and 400 nM of protein. Then, 3 nM of 3′ overhang DNA was added to the reactions and incubated for 10 min at 30°C. After deproteinization, by incubation with 0.1% SDS and 500 μg/ml of proteinase K at 30°C for 3 min, reactions were resolved by 12% native PAGE and the gel was scanned with a Fuji FLA 9000 imager (Fuji).

Sensitivity spot assay

Cells were grown to mid- to late-log phase in YPD and diluted in water to $OD_{600} \sim 0.2$. Several 10-fold serial dilutions were spotted on a YPD plate supplemented with CPT (0.5, 1 and 2 μg/ml), HU (25, 50 and 100 mM), MMS (0.005, 0.01 and 0.02%) or Zeocin (2.5 and 5 μg/ml). Drugs were added to the agar medium just before pouring the plates. Pictures of the plates were taken after 2 days incubation at 30°C.

Fluorescent microscopy

Yeast cells were grown and processed for fluorescence microscopy as described previously (45) and imaged at 25°C. Fluorophores were visualized on a DeltaVisionElite microscope (Applied Precision, Inc) equipped with a 100x objective lens (Olympus U-PLAN S-APO, NA 1.4), a cooled Evolve 512 EMCCD camera (Photometrics, Japan), and Insight solid state illumination source (Applied Precision, Inc). Pictures were processed with Volocity software (PerkinElmer). Images were acquired using softWoRx (Applied Precision, Inc) software.

RESULTS

Residues 783–860 of Srs2 interact with Mus81

Genetic studies in yeast have previously implicated Srs2 and Mus81 in the repair of single-stranded gaps, where Srs2 channels the intermediate into the Mus81 sub-pathway (18,46). In order to ascertain a sub-pathway of repair that is dependent on the activities of both Srs2 and Mus81, we tested for a direct interaction between Srs2 and Mus81 using pull-down assays with a purified Srs2 (His-$Srs2^{1–1174}$) and V5-His-Mus81. When applied to anti-V5 agarose beads, Mus81 was able to retain full-length Srs2 (Figure 1C, lanes 1–4). Next, we also tested whether Srs2 could co-precipitate Mus81 from yeast. Extract from yeast cells expressing His-Mus81 was incubated in the presence or absence of purified GST-$Srs2^{783–998}$ followed by pull-down using GSH-beads. Immunoblotting of the supernatant as well as the elution fractions with anti-His antibody confirmed the ability of Srs2 to bind Mus81 (Figure 1D).

In order to map the Mus81 interaction domain within Srs2, we constructed and purified several N-terminal Srs2 truncations (Figure 1B). To test the interaction with Mus81, we mixed two truncations ($Srs2^{1–898}$ or $Srs2^{1–860}$) with V5-His-Mus81 and anti-V5 agarose beads. Both Srs2 variants were retained on the beads (Figure 1C), suggesting that the last 300 amino acids, including PCNA and Rad51 binding domains are not necessary for the interaction with Mus81 protein. In addition, this experiment confirmed that the interaction is independent of the GST-tag. To further narrow

Downloaded from http://nar.oxfordjournals.org/ at Danmarks NaturOG on May 2, 2016

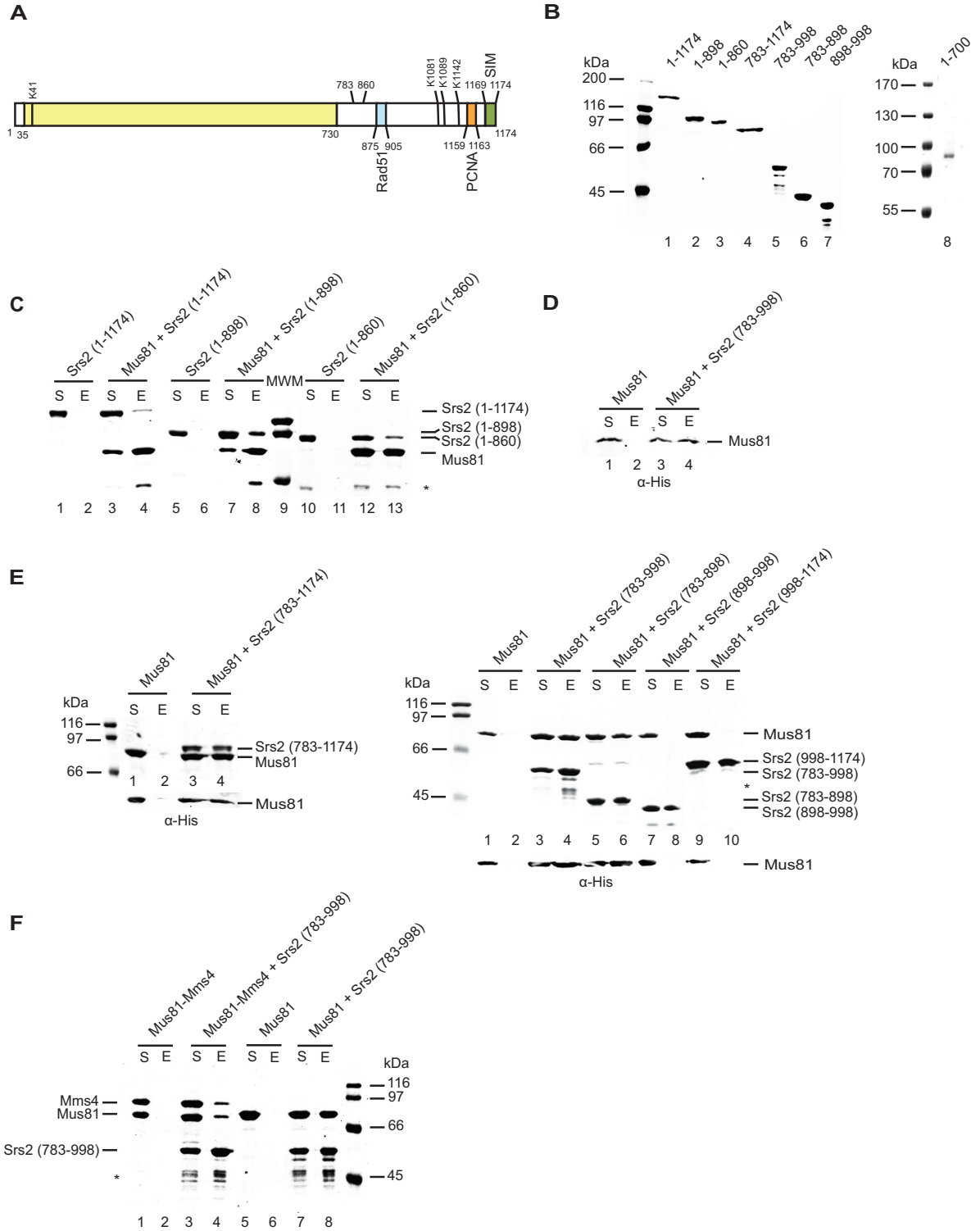

Figure 1. Srs2 physically interacts with Mus81 and Mus81–Mms4. **(A)** Schematic illustration of the domains within Srs2. **(B)** Purified Srs2 (lane 1), $Srs2^{1–898}$ (lane 2), $Srs2^{1–860}$ (lane 3), GST-$Srs2^{783–1174}$ (lane 4), GST-$Srs2^{783–998}$ (lane 5), GST-$Srs2^{783–898}$ (lane 6), GST-$Srs2^{898–998}$ (lane 7) and $Srs2^{1–700}$ (lane 8) used in the study were resolved by SDS-PAGE and stained with Coomassie blue. **(C)** Full-length Srs2 (5 μg, lanes 1–4), $Srs2^{1–898}$ (lanes 5–8) and $Srs2^{1–860}$ (lanes 10–13) were incubated with anti-V5 agarose beads either alone or in the presence of Mus81 (5 μg). The beads were incubated, washed and treated with SDS to elute bound proteins. The supernatant (S) and eluate (E) fractions were analyzed by Coomassie blue staining. The asterisk shows protein contamination. **(D)** Yeast extract containing His-Mus81 was incubated with GSH-beads alone (lanes 1 and 2) or with purified GST-$Srs2^{783–998}$ (lanes 3 and 4). After incubation, supernatants and beads were analyzed by western blot with anti-His antibodies to detect the presence of Mus81 protein. **(E)** Mus81 (5 μg) was mixed with GSH-beads either in the absence (lanes 1 and 2) or presence of the indicated GST fragments of Srs2 (5 μg; lanes 3–10). The products were analyzed as in (C). The asterisk indicates protein degradation. **(F)** Mus81–Mms4 (5 μg) or Mus81 (5 μg) were mixed with GSH-beads in the presence or absence of GST-$Srs2^{783–998}$ (5 μg). Beads were analyzed as in (C) above. The asterisk indicates protein degradation.

Downloaded from http://nar.oxfordjournals.org/ at Danmarks NaturOG on May 2, 2016

down the interaction domain, we constructed and purified five additional C-terminal truncations of Srs2, including GST-Srs2$^{783–1174}$, GST-Srs2$^{783–998}$, GST-Srs2$^{783–898}$, GST-Srs2$^{898–998}$ and GST-Srs2$^{998–1174}$. These fragments of Srs2 were mixed with Mus81 and incubated with GSH-beads. As shown in Figure 1E, only fragments GST-Srs2$^{898–998}$ and GST-Srs2$^{998–1174}$ failed to bind Mus81 protein, as confirmed by Coomassie blue staining as well as western blot analysis. Finally, we also tested the ability of Srs2 to interact with the Mus81 subunit or the Mus81–Mms4 complex. When applied to GSH-beads, GST-Srs2 was able to retain both the Mus81–Mms4 complex as well as Mus81 alone (Figure 1F). In summary, these experiments indicate a direct physical interaction between Srs2 and the Mus81–Mms4 complex. This interaction is mediated via Mus81 and the region responsible for this interaction within Srs2 protein resides in aa 783–860.

The N-terminus of Mus81 is required for interaction with Srs2

Since the Mus81 protein mediates the interaction with Srs2, we aimed to determine the region of Mus81 protein required for this interaction. We therefore cloned, expressed and purified an N-terminal fragment of Mus81 (V5-His-Mus81$^{1–319}$) and tested its interaction with full-length Srs2. A C-terminal fragment of Mus81 (V5-His-Mus81$^{319–632}$) was insoluble and could not be used for the analysis. As shown in Figure 2A, the N-terminus of Mus81 was able to retain Srs2 on anti-V5 agarose beads. In addition, we compared the binding between full-length Mus81 and Mus81$^{1–319}$ and found that they both bind the Srs2 (Supplementary Figure S1A). Next, we tested the affinity of Mus81$^{1–319}$ toward various N- and C-terminal truncations of Srs2. Using the GSH-bead pull-down assay, an identical pattern of interaction was observed with full-length Mus81. Similar results were obtained using both Coomassie blue staining and western blot analysis. The inability of the Srs2$^{1–700}$ fragment to interact with Mus81$^{1–319}$ confirms that the interaction domain within Srs2 resides between aa 783–860 (Figure 2B, C and D).

To map the interaction domain in greater details we took advantage of the yeast two-hybrid assay. Here, the Srs2$^{783–1174}$ fragment was cloned into the pGADT7 vector and transformed into strain PJ69a. Next different truncations of Mus81 (Mus81$^{1–155}$, Mus81$^{1–220}$, Mus81$^{1–245}$, Mus81$^{1–288}$, Mus81$^{138–632}$, Mus81$^{290–632}$) cloned into pGBKT7 were transformed into the PJ69α strain. Corresponding strains were mated and grown on SD/-His/-Trp/-Leu to select for positive interactions. As shown in Figure 2E and Supplementary Figure S1B, the shortest Mus81 fragment interacting with Srs2 contains the region 1–155. Taken together, we conclude that the Srs2-interacting domain is located within the first 155 amino acids of Mus81.

Srs2 stimulates the activity of the Mus81–Mms4 endonuclease

We (42) and others (47,48) have demonstrated that physical interactions with other proteins can lead to stimulation of Mus81–Mms4 nuclease activity. Therefore, we asked whether Srs2 had any effect on the endonuclease activity of the Mus81–Mms4 complex. First, we used a 3′-flap DNA structure which is one of the Mus81–Mms4's preferred substrates and a relevant DNA intermediate during DNA repair and replication (27). We titrated full-length Srs2 together with an amount of Mus81–Mms4 that cleaves ∼10% of the substrate (0.25 nM). Indeed, we observed robust stimulation of the Mus81–Mms4 endonuclease activity by Srs2 (Figure 3A). In particular, the cleavage was stimulated ∼2-fold by 5 nM, 4-fold by 10 nM and 8-fold when 80 nM of Srs2 was added to the reaction (Figure 3B). This stimulation did not change the cleavage pattern of Mus81–Mms4 as seen on denaturing PAGE (Supplementary Figure S1C).

In addition, we wished to test whether Srs2 was able to target Mus81–Mms4 to the substrate. To this end, preincubation of Srs2 with 3′-flap DNA substrate followed by addition of Mus81–Mms4 resulted in 3- to 4-fold higher stimulation of nuclease activity compared to a reaction in which both proteins were added simultaneously (Figure 3C and D). To further characterize the effect of Srs2 on the rate of Mus81–Mms4 cleavage, we conducted time course experiments. A sub-optimal amount of Mus81–Mms4 complex (0.25 nM) was incubated either alone or with 10 nM Srs2 in the presence of 3′-flap DNA, and aliquots of the reaction were withdrawn and analyzed over time. As shown in Figure 3E and F, in the presence of 10 nM Srs2 resulted in a 2-fold stimulation of 3′-flap cleavage in the first 10 min, and a maximum of 6-fold stimulation at 50 min compared to the Mus81–Mms4 reaction alone.

Next, we tested whether various truncation fragments of Srs2 could also stimulate Mus81–Mms4 activity. Increasing concentrations of each fragment and full-length Srs2 protein were mixed together with the Mus81–Mms4 complex (0.25 nM) and the 3′-flap structure. As expected, all Srs2 fragments that interacted with Mus81 in pull-down assays were also able to stimulate Mus81–Mms4 nuclease activity. In particular, the Srs2$^{1–898}$, Srs2$^{1–860}$ and Srs2$^{783–1174}$ truncations containing region 783–860 of Srs2 were able to stimulate nuclease cleavage to the same extent as full-length Srs2 (Figure 3G and H). Although decreased, Srs2$^{783–898}$ was also able to significantly stimulate the Mus81–Mms4 complex. Figure 3G summarizes the quantification of the individual experiments. We also tested if Srs2$^{1–700}$ was able to stimulate nuclease activity of Mus81–Mms4 since it failed to interact. We observed only mild stimulation compared to full-length Srs2 (Supplementary Figure S1D and E). Similarly, the Srs2$^{898–998}$ and Srs2$^{998–1174}$ fragments showed very mild stimulation of 3′-flap cleavage and only at the highest concentration used (Figure 3G). In addition we also created an Srs2 mutant missing the Mus81-interaction domain (Srs2-Δ783–860). However, this mutant had poor solubility and lacked both Mus81–Mms4 stimulation and DNA helicase activity. The fact that these results were obtained despite the fact that Srs2-Δ783–860 contains all helicase domains, suggested a potential misfolding or instability defect (data not shown). For this reason, Srs2-Δ783–860 was not used for further analysis.

Srs2 possesses a ssDNA-dependent ATPase activity (5,49). This activity fuels its translocation on ssDNA thus allowing the unwinding of DNA as well as disassembly of Rad51-ssDNA nucleoprotein filaments (8–9,49). The Srs2-

Downloaded from http://nar.oxfordjournals.org/ at Danmarks NaturOG on May 2, 2016

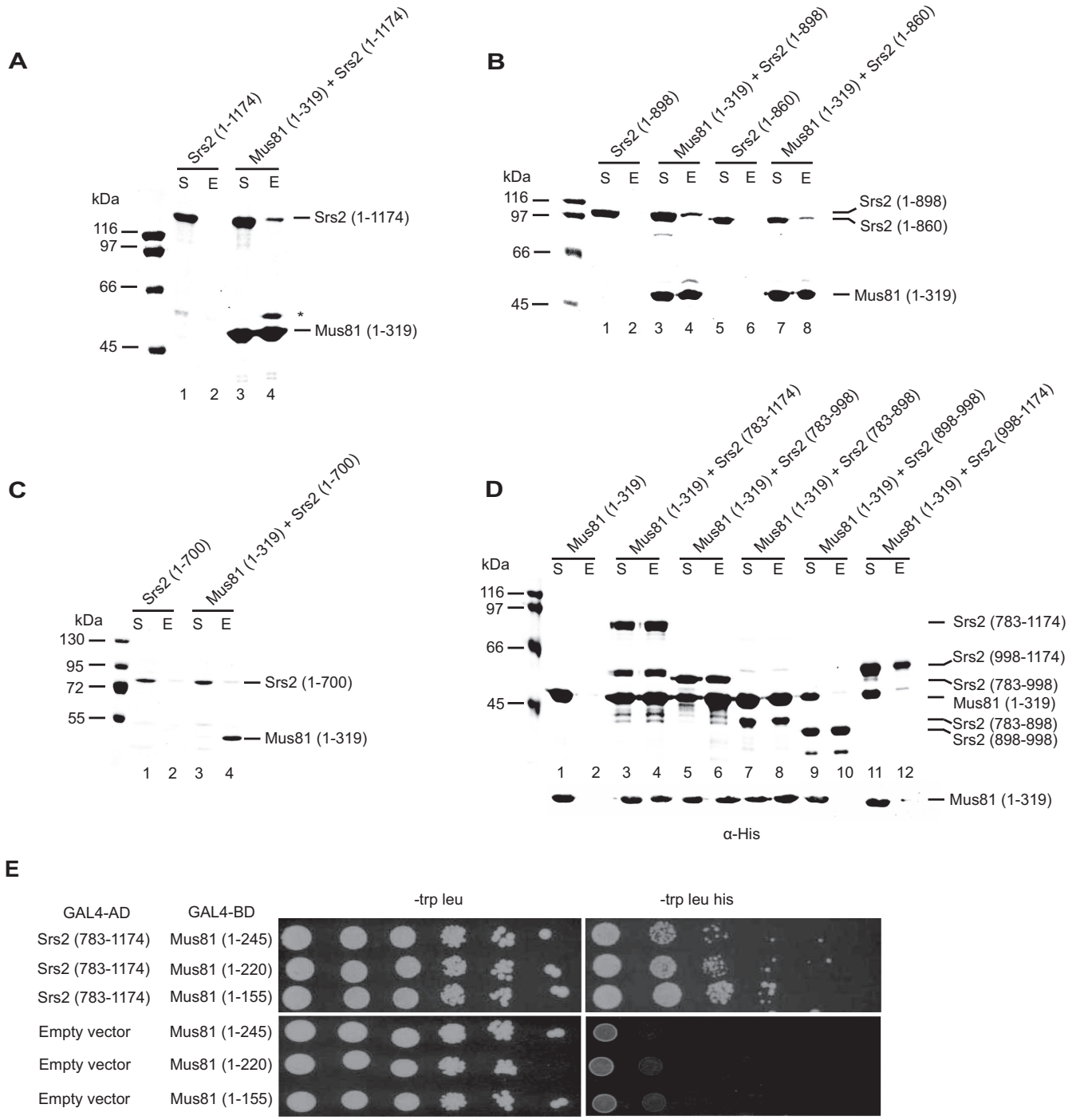

Figure 2. Mapping of the Srs2 interaction with Mus81. **(A)** Full-length Srs2 (5 μg) was incubated in the absence or presence of $Mus81^{1–319}$ (5 μg) and anti-V5 agarose beads. Beads were washed, treated with SDS to elute bound proteins and fractions analyzed by Coomassie blue staining. The asterisk shows protein contamination. **(B)** $Srs2^{1–898}$ (5 μg, lanes 1–4) and $Srs2^{1–860}$ (lanes 5–6) were mixed with $Mus81^{1–319}$ (5 μg) as indicated, followed by incubation with anti-V5 agarose beads. Beads were treated as described above. **(C)** $Srs2^{1–700}$ (5 μg) was incubated in the absence or presence of $Mus81^{1–319}$ (5 μg) and anti-V5 agarose beads. Beads were analyzed as described above. **(D)** $Mus81^{1–319}$ (5 μg) was mixed with GSH-beads (lanes 1 and 2) or with GST-$Srs2^{783–1174}$, -$Srs2^{783–998}$, -$Srs2^{783–898}$, -$Srs2^{898–998}$, or -$Srs2^{998–1174}$ (5 μg) and GSH-beads (lanes 3–12). The beads were treated as described above. **(E)** The yeast two-hybrid interaction between Srs2 and Mus81 is mediated by the N-terminus of Mus81. Strain PJ69–4 containing indicated plasmids expressing Srs2 fused to the GAL4 transcription activation domain and N-terminal regions of Mus81 ($Mus81^{1–155}$, $Mus81^{1–220}$ and $Mus81^{1–245}$) fused to the GAL4 DNA-binding domain were spotted as 10-fold serial dilutions on medium lacking tryptophan and leucine (-trp leu) or lacking tryptophan, leucine and histidine (-trp leu his). The empty vector (pGADT7) was included as negative control.

Downloaded from http://nar.oxfordjournals.org/ at Danmarks NaturOG on May 2, 2016

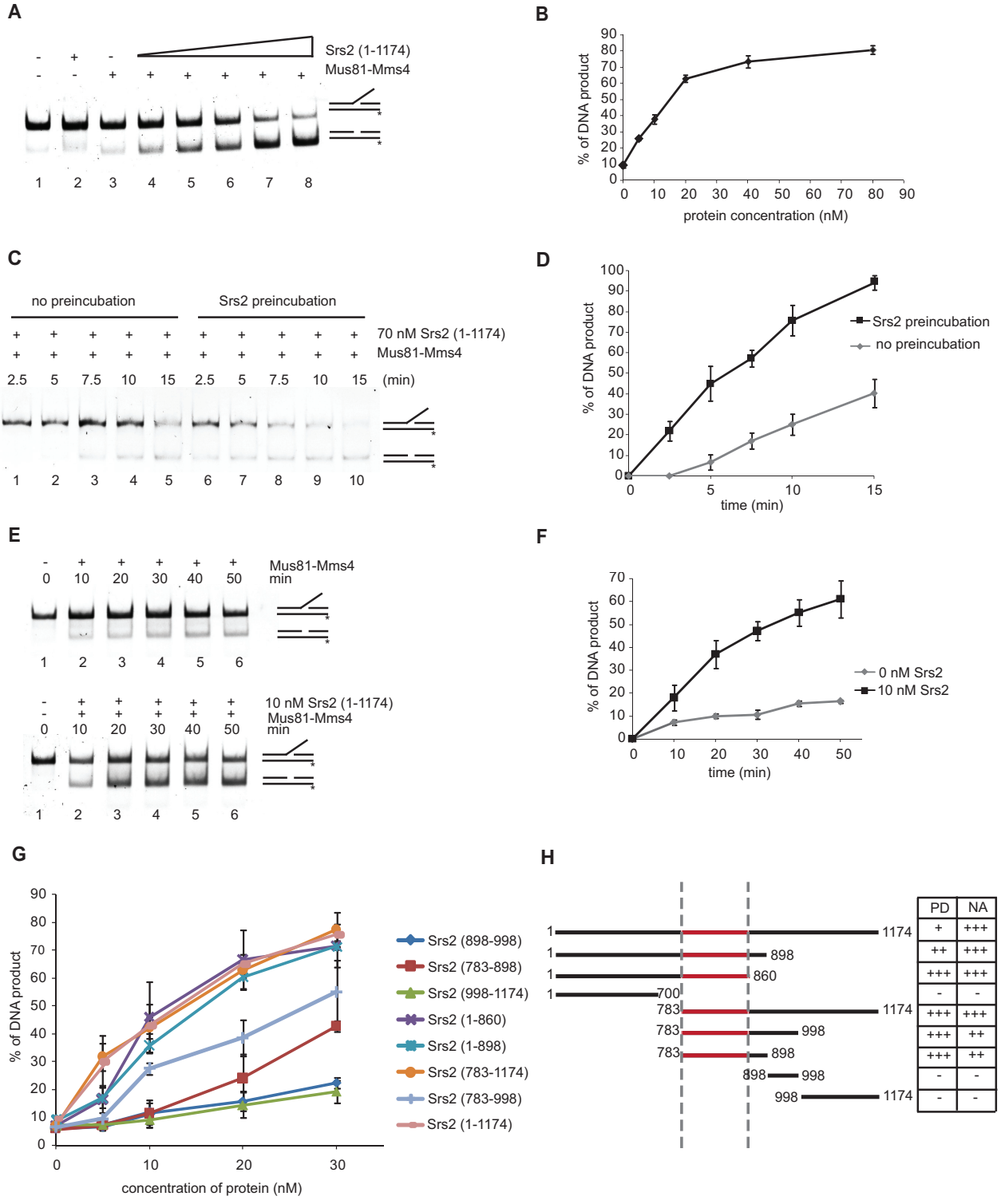

Figure 3. Srs2 stimulates Mus81–Mms4 nuclease activity. **(A)** Mus81–Mms4 (0.25 nM) and increasing amounts of Srs2 (5, 10, 20, 40 and 80 nM) were first pre-incubated at 30°C for 30 min followed by addition of 3'-flap DNA substrate (7 nM) and incubation for 30 min at 37°C prior to analysis by native gel electrophoresis. **(B)** Quantification of the data in (A) with S.D. based on three independent experiments. **(C)** Srs2 targets Mus81–Mms4 complex for cleavage. Srs2 (70 nM) was first pre-incubated with 3′-flap structure (6 nM) at 30°C for 10 min followed by the addition of Mus81–Mms4 (0.25 nM) and incubation for 2.5, 5, 7.5, 10 and 15 min at 30°C. Corresponding aliquots were analyzed as in (A). **(D)** Quantification of the data in (C) from a minimum of three independent experiments. **(E)** Mus81–Mms4 (0.25 nM) was incubated with 3'-flap DNA (7 nM) in the absence or presence of Srs2 (10 nM) at 37°C for 10, 20, 30, 40 and 50 min. Aliquots of the reactions were taken at the indicated times and analyzed as in (A). **(F)** Quantification of the data in (E) with S.D. based on three independent experiments. **(G)** Quantification of nuclease assays with various fragments of Srs2 with S.D. based on three independent experiments. **(H)** Summary of interaction mapping by pull-down (PD) and nuclease assays (NA).

Downloaded from http://nar.oxfordjournals.org/ at Danmarks NaturOG on May 2, 2016

K41R protein, which contains a mutation in the Walker A domain that is responsible for the binding and hydrolysis of ATP, is devoid of the above-mentioned functions (50). We therefore next asked if this mutant is able to stimulate the endonuclease activity of the Mus81–Mms4 complex. For that purpose we performed nuclease assays in the presence of the increasing amounts of Srs2-K41R. As shown in the Supplementary Figure S2A, Srs2-K41R protein is fully capable of stimulating Mus81–Mms4 to the same extent as wild-type Srs2. This indicates that the helicase activity of Srs2 is not required for the stimulation of the Mus81–Mms4 complex. To further support this conclusion, we tested the ability of ATP-γ-S to potentiate the stimulatory effect of Srs2 on the Mus81–Mms4 nuclease activity. However, ATP-γ-S had no effect on the stimulation of Mus81–Mms4 by Srs2 (Supplementary Figure S2B).

In summary, these data indicate that Srs2 is able to efficiently stimulate the nuclease activity of Mus81–Mms4. We conclude that the region 783–860 of Srs2 is required for both Mus81 interaction and stimulation, and that this stimulation is independent of Srs2 helicase/ATPase activity.

Stimulation of Mus81–Mms4 activity by Srs2 is species-specific

Due to the evolutionary conservation of Mus81 protein, we also tested the effect of Srs2 on the human MUS81 homolog. First, we analyzed the ability of GST-Srs2$^{783–998}$ to interact with the human MUS81–EME1 complex. Using a pull-down assay we observed MUS81–EME1 binding to GSH-beads in the presence of a GST-Srs2 fragment (Supplementary Figure S3A), which indicates that they physically interact. Using the same approach as above, we then tested the effect of Srs2 on MUS81–EME1 nuclease activity. However, Srs2 showed only limited enhancement of human MUS81–EME1 activity compared to the robust stimulation of yeast Mus81–Mms4 (Supplementary Figure S3B). This indicates that despite the observed interaction, it is insufficient to stimulate MUS81–EME1 nuclease activity. To further analyze the specificity of the stimulation, we also tested the effect of Srs2 on another structure-specific nuclease, the yeast Rad1–Rad10 complex. In contrast to Mus81–Mms4, addition of Srs2 did not result in significant stimulation; rather, we observed inhibition at higher Srs2 protein concentration (Supplementary Figure S3C). Similarly, we did not observe stimulation of Mus81–Mms4 nuclease activity by UvrD helicase, the bacterial homolog of Srs2 (Supplementary Figure S3D), which confirms the specificity of Srs2 stimulation toward Mus81–Mms4.

Cleavage of D-loop, nicked HJ and fork structures is also stimulated by Srs2

Mus81–Mms4 was previously shown to cleave a number of DNA structures including those resembling replication forks, nicked Holliday junctions (nHJ) D-loops and 3′-flaps, whereas Y form and intact HJs were not efficiently cleaved (25–27). We therefore wanted to test whether Srs2 could also stimulate the endonuclease activity of Mus81–Mms4 on other substrates. As shown in Supplementary Figure S4, Srs2 was efficient in stimulating Mus81–Mms4 cleavage of D-loops, nHJ and fork DNA substrates to the same extent as the 3′-flap DNA structure. On the other hand, we did not observe any stimulation of Mus81–Mms4 nuclease activity on Y form DNA (Supplementary Figure S4C), indicating that Srs2 can modulate its activity but not influence the structure selectivity of Mus81. Altogether, Srs2 is capable of dramatically stimulating the nuclease activity of Mus81–Mms4 on all substrates that this complex cleaves.

Effect of Mus81–Mms4 on the helicase activity of Srs2

The ability of Srs2 to stimulate the nuclease activity of the Mus81–Mms4 complex prompted us to also test the effect of Mus81 on Srs2 helicase activity. We pre-incubated Srs2 with increasing concentrations of Mus81–Mms4 complex and monitored the unwinding of a 3′ overhang DNA structure. This substrate was chosen to avoid the nuclease activity of the Mus81–Mms4 complex. As shown in Figure 4A, an equimolar amount of Mus81–Mms4 results in almost 20% inhibition of Srs2 helicase activity while 60% inhibition was observed with 300 nM of the Mus81–Mms4 complex. Since the interaction between Srs2 and Mus81–Mms4 is mediated by Mus81 protein, we next tested whether Mus81 alone or its N-terminal domain (Mus81$^{1–319}$) was also able to inhibit Srs2 helicase activity. Both Mus81 and Mus81$^{1–319}$ inhibited Srs2 helicase to the same extent as Mus81–Mms4 complex (Figure 4B and C). To test the specificity of this inhibition, we performed the same helicase assay with another Srs2-interacting protein, Mre11. In contrast to Mus81, our results show that Mre11 was not able to block Srs2 helicase activity (Figure 4D), confirming the specificity of Mus81 inhibition.

Rad51 inhibits cleavage by Mus81–Mms4 in a reaction suppressed by Srs2

Since some of the structures that the Mus81–Mms4 complex is able to cleave arise during recombination, we asked whether the presence of Rad51 on such DNA will influence the nuclease activity. Hence, we pre-incubated 3′-flap DNA with increasing concentrations of Rad51 before addition of Mus81–Mms4 complex. As shown in Figure 5A (lanes 4–8), addition of Rad51 results in inhibition of Mus81–Mms4 nuclease activity. As expected, full inhibition was observed approximately at saturation of the ssDNA part of the substrate (3:1 nucleotide:monomer).

The ability of Srs2 to inhibit Rad51-mediated recombination by dismantling the Rad51-ssDNA presynaptic filament (8,9) prompted us to test whether this activity of Srs2 can suppress Rad51-mediated inhibition of Mus81–Mms4 nuclease activity. Therefore, we pre-incubated Rad51 (600 nM) with 3′-flap DNA followed by addition of Mus81–Mms4 (0.4 nM) and increasing concentrations of Srs2. While the Rad51-filament formation inhibited the nuclease activity, addition of Srs2 resulted in suppression of the Rad51-mediated inhibition of Mus81–Mms4 activity (Figure 5B). In particular, 5 nM Srs2 resulted in a 2-fold increase, and 20 nM Srs2 in a 5-fold increase of Mus81–Mms4 activity compared to the inhibited reaction (Figure 5C). To determine whether the suppression of Rad51 inhibition was due to its removal from the DNA by Srs2, we also tested the effect of the Srs2-K41R mutant. As expected, Srs2-K41R was

Downloaded from http://nar.oxfordjournals.org/ at Danmarks NaturOG on May 2, 2016

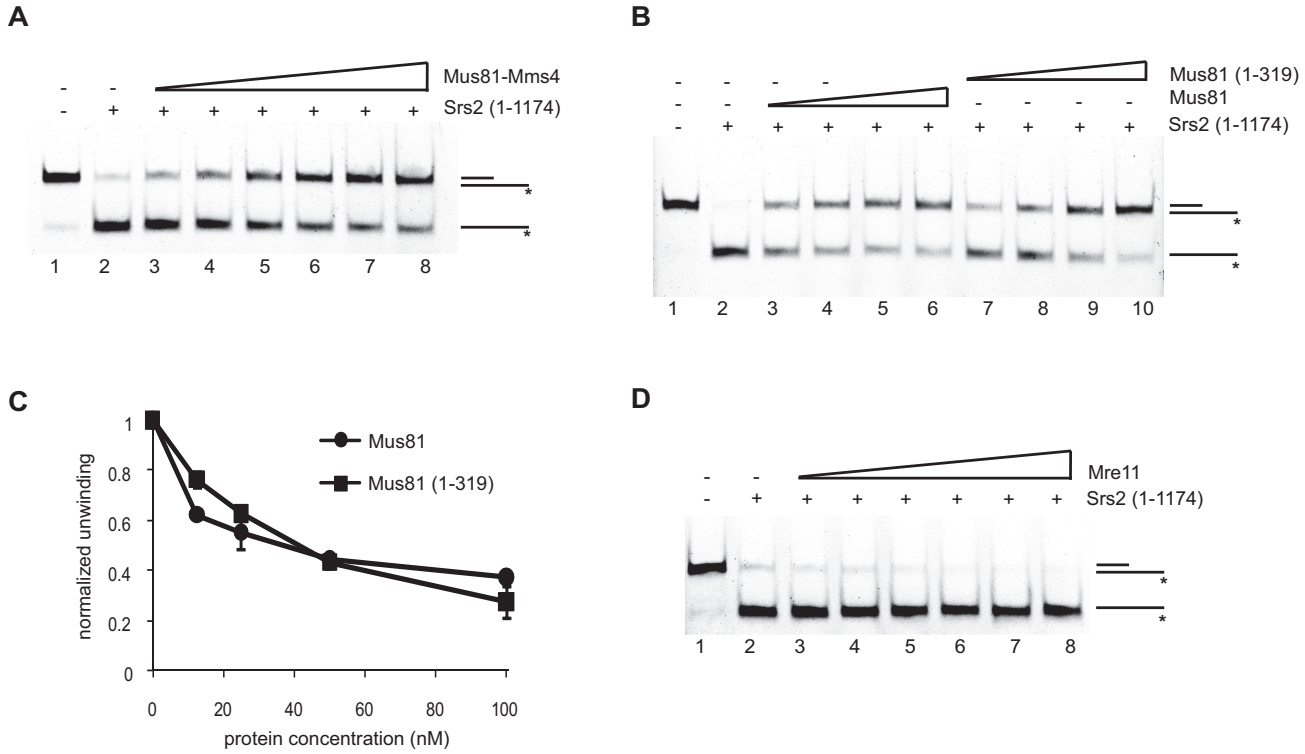

Figure 4. Mus81 blocks Srs2 helicase activity. **(A)** Srs2 (10 nM) was incubated with Mus81–Mms4 (12.5, 25, 50, 100, 200 and 300 nM) on ice for 10 min. The 3′ overhang DNA (3 nM) was then added to the reactions and incubated for 10 min at 30°C prior to analysis by native gel elctrophoresis. **(B)** Srs2 (10 nM) was indicated with either Mus81 or Mus81$^{1–319}$ fragment (12.5, 25, 50 and 100 nM) on ice. The 3′ overhang DNA (3 nM) was then added, and the reactions were incubated for 10 min at 30°C prior to gel analysis as above. **(C)** Quantification of the data in (B) with S.D. based on three independent experiments. **(D)** Srs2 (10 nM) was incubated with increasing concentrations of Mre11 (12.5, 25, 50, 100, 200, 300 and 400 nM). After addition of substrate DNA, the reactions were incubated for 10 min at 30°C and analyzed as above.

not able to alleviate the effect of Rad51 on Mus81–Mms4 cleavage (Figure 5D), indicating that translocation of Srs2 and removal of Rad51 is required for this activity.

Genetic interactions between *MUS81* and *SRS2*

Previous genetic data in budding and fission yeast suggests that Srs2 and Mus81 act in the repair of single-stranded gaps (18,46). To further assess the roles of the *SRS2* and *MUS81* genes, we spotted dilutions of wild-type, single and double deletion mutant strains onto agar plates containing the ribonucleotide reductase inhibitor HU, the alkylating agent MMS, the topoisomerase I poison CPT and the radiomimetic chemical Zeocin. As shown in Figure 6, the double mutant was more sensitive to several of these agents than either single mutant. The fact that this occurred at the lowest concentrations of CPT, HU and MMS is consistent with the idea that Mus81 and Srs2 act in separate parallel pathways for the processing of DNA damage induced by these agents.

The synergistic effect observed in the double mutant might be due to the multifunctional role of Srs2 in various DNA repair pathways. Therefore, we also tested the *srs2-K41R* mutant strain that is unable to remove Rad51 from ssDNA (50). The *srs2-K41R mus81* deletion strain showed even greater sensitivity to CPT, HU and Zeocin compared to the double deletion mutant. This suggests that the ability to remove Rad51 and/or unwind recombination intermediates is also a Mus81-independent function.

Mus81 and Srs2 co-localize after DNA damage

Our biochemical data prompted us to test whether Srs2 and Mus81 co-localize *in vivo* with or without DNA damage. Only ∼9% of the budded cells contained spontaneous Mus81 foci and this formation was induced up to 20% by treatment with CPT or Zeocin. In contrast, treatment of the cells with HU had no significant effect on Mus81 focus formation (Figure 7). Accordingly, we observed significant co-localization of Srs2 and Mus81 foci after treatment with CPT, indicating a role for these proteins in the repair of CPT-induced damage (Figure 7). The co-localization of Mus81 and Srs2 after Zeocin treatment is also significant and was further enhanced by prolonged treatment (Figure 7B), suggesting that Srs2 and Mus81 function together in the repair of chromosome damage. Analysis of cell cycle stage shows culmination of Srs2 foci in S/G2, co-localization foci with Mus81 in G2 and Mus81 foci alone in G2/M phase (Figure 7C), suggesting that Srs2 might be responsible for targeting Mus81 to sites of DNA repair. However, Mus81 was fully proficient in focus formation in the absence of Srs2 (Supplementary Figure S5). Further, there was a statistically significant increase in spontaneous Mus81 foci in the *srs2* strain that was further increased

Downloaded from http://nar.oxfordjournals.org/ at Danmarks NaturOG on May 2, 2016

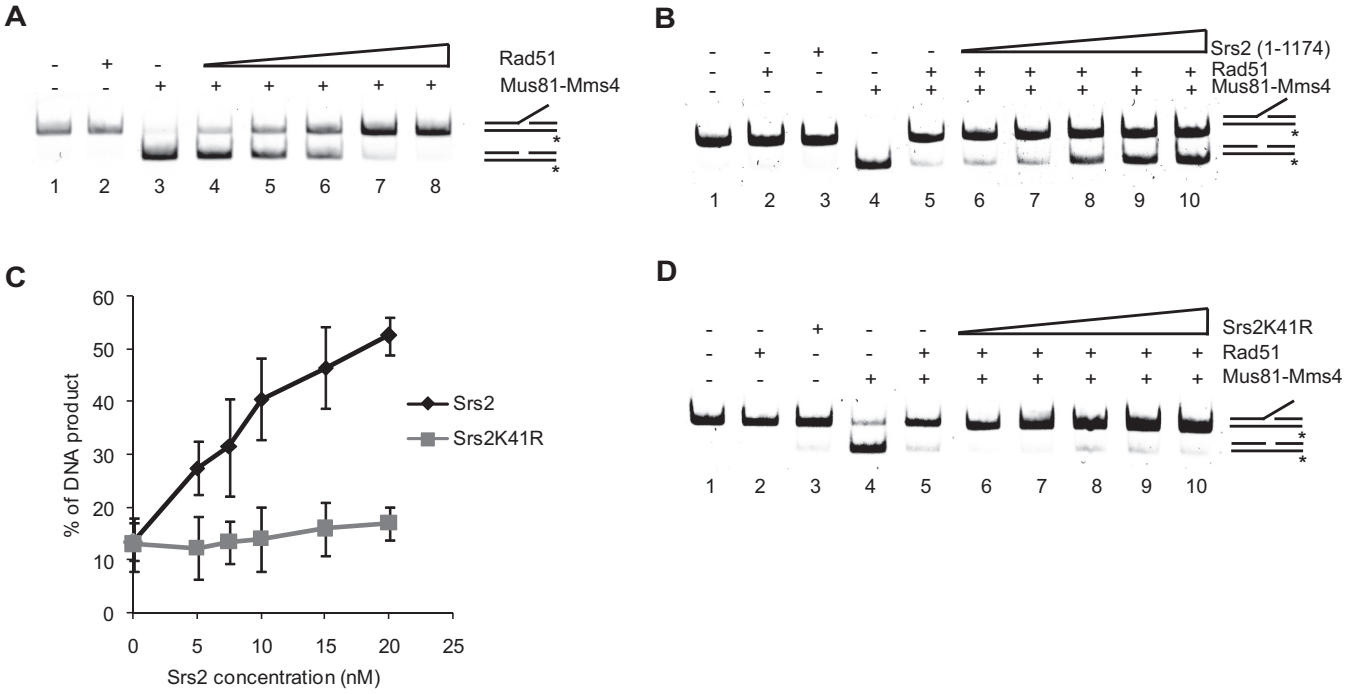

Figure 5. Rad51 inhibits Mus81–Mms4 nuclease activity. **(A)** The 3′-flap DNA (7 nM) was incubated with Rad51 (100, 200, 400, 600 and 800 nM) for 10 min at 37°C. Mus81–Mms4 (0.4 nM) was then added to the mixture and the reaction was further incubated for 30 min at 37°C and analyzed as in Figure 3A. **(B)** The reaction was assembled as described above with 600 nM Rad51 being pre-incubated with DNA. Mus81–Mms4 along with increasing concentrations of Srs2 (5, 7.5, 10, 15 and 20 nM) were added to the reaction, incubated for additional 30 min at 37°C and analyzed as above. **(C)** Quantification of the data in (B) and (D) with S.D. based on three different experiments. **(D)** The 3′-flap DNA (7 nM) was incubated with Rad51 (600 nM) for 10 min at 37°C followed by addition of Mus81–Mms4 (0.4 nM) and Srs2-K41R (5, 7.5, 10, 15 and 20 nM). The reactions were incubated for 30 min at 37°C and analyzed.

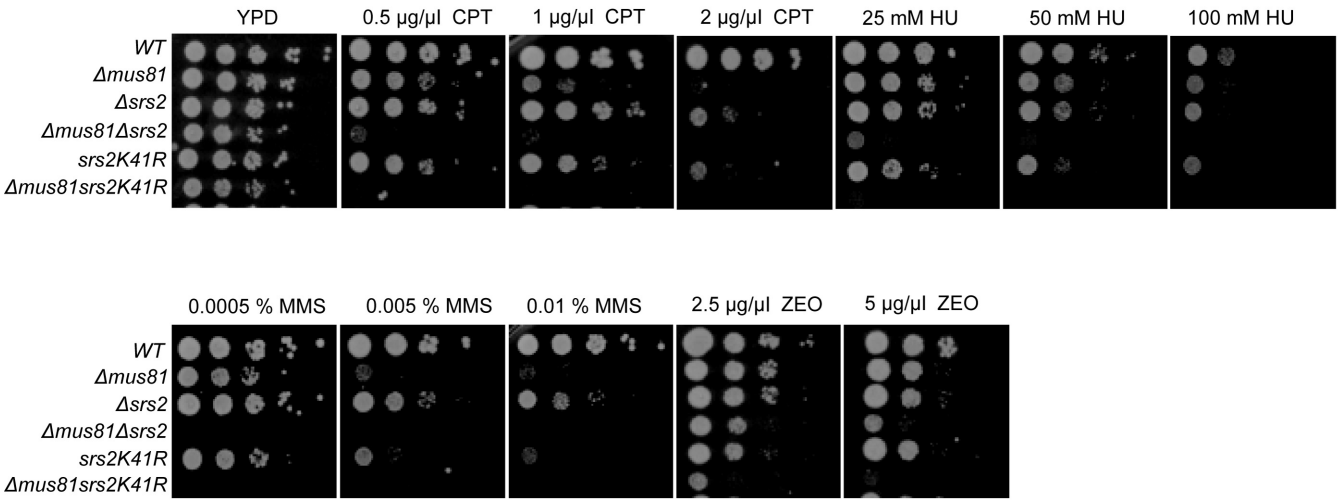

Figure 6. Genetic interactions between Srs2 and Mus81. DNA damage sensitivity of wild type (WT), *mus81Δ*, *srs2Δ*, *srs2-K41R* and the indicated double mutants was assayed by spotting 10-fold serial dilutions of each strain on YPD plates and plates containing the indicated concentrations of CPT, HU, MMS and Zeocin.

upon DNA damage. Such a result is consistent with the idea that this strain accumulates toxic recombination intermediates that are targets for Srs2-independent recruitment of Mus81. Taken together, these results are consistent with DNA damage-induced co-localization of Mus81 and Srs2. The fact that Srs2 focus formation precedes Mus81 suggests that Srs2 could play a role in its regulation at the site of repair.

DISCUSSION

The structure-specific endonuclease Mus81–Mms4/Eme1 has been shown to be involved in the maintenance of

Downloaded from http://nar.oxfordjournals.org/ at Danmarks NaturOG on May 2, 2016

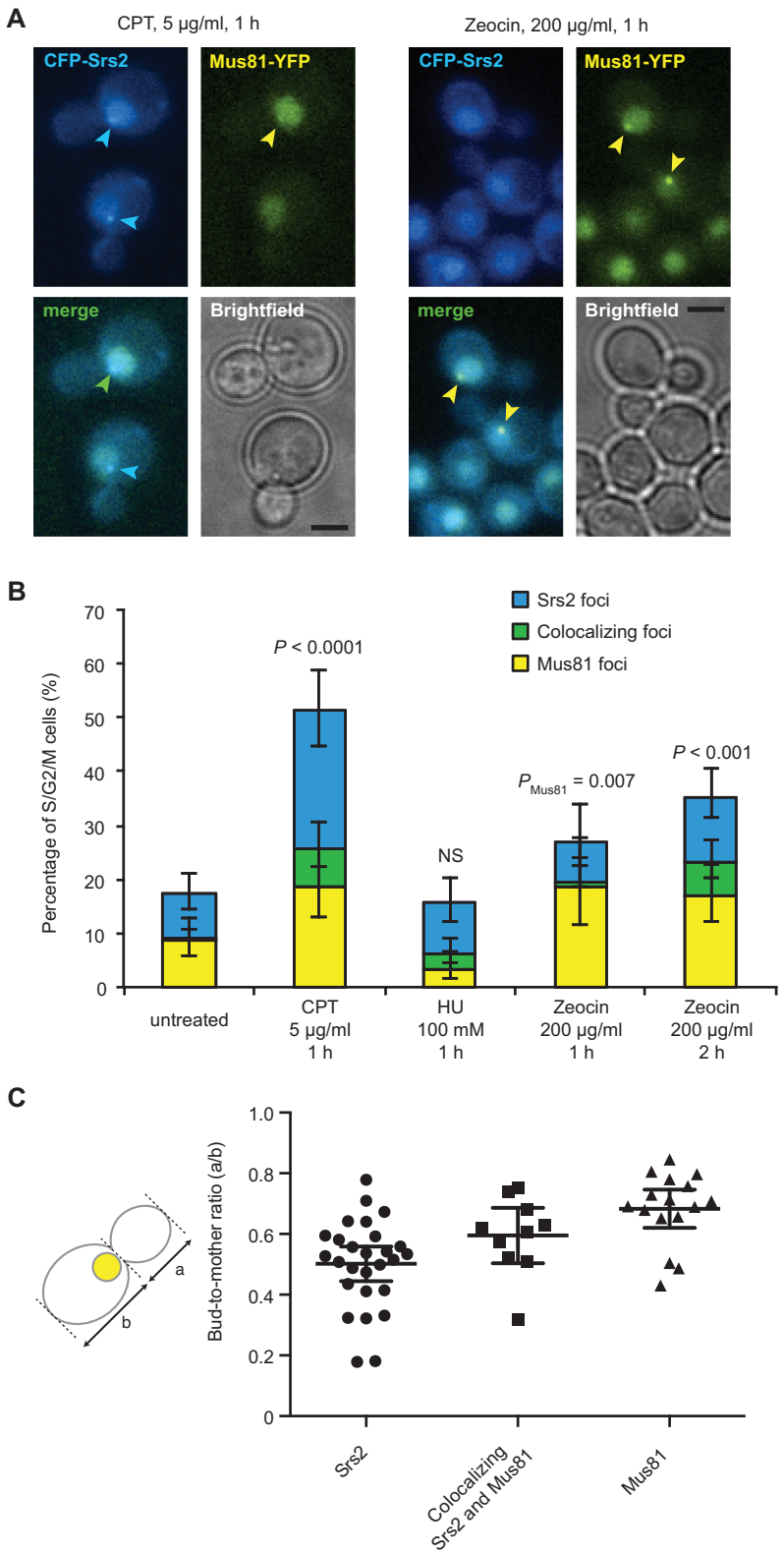

Figure 7. Localization of Srs2 and Mus81 after DNA damage. Cells expressing CFP-Srs2 and Mus81-YFP (ML733–12C) from their endogenous loci were grown to exponential phase in synthetic complete medium supplemented with 100 µg/ml adenine at 25°C and subjected to fluorescence microscopy before and after treatment with CPT, HU or Zeocin. **(A)** Srs2 and Mus81 co-localize at a subset of DNA lesions. Shown are images of representative cells after CPT and Zeocin treatment. Arrowheads indicate foci. Scale bar, 3 µm. **(B)** Quantification of Srs2 and Mus81 foci. For each experimental condition 300–600 cells were examined. Error bars indicate 95% confidence intervals. Significance relative to the untreated condition was determined by Fisher's exact test. NS, not significant. **(C)** Cell cycle distribution of Srs2 and Mus81 foci. For the CPT treated cells in panel B, cell cycle phase was evaluated by measuring the bud-to-mother size ratio. Error bars represent 95% confidence intervals.

Downloaded from http://nar.oxfordjournals.org/ at Danmarks NaturOG on May 2, 2016

genome integrity by processing replication, recombination and repair intermediates (22,29,31,51–52). Mounting evidence also points to multiple roles of Srs2 during DNA replication and recombination (4). Despite the roles of Srs2 and Mus81 in SDSA, and recent advances in understanding their regulation, the molecular mechanism of these enzymes remains unclear. Here, we demonstrate a direct physical interaction between Srs2 and the Mus81–Mms4 complex *in vitro* as well as their co-localization *in vivo*. We also show that this association leads to a strong stimulation of Mus81–Mms4 nuclease activity on a variety of substrates. Together, these findings lead us propose a model where, despite their independent roles, Srs2 and Mus81 cooperate in the resolution of replication and recombination intermediates to ensure genome stability.

Several pieces of evidence support this idea. First, the N-terminus of Mus81 mediates the direct physical interaction with Srs2, while the Mus81-interaction domain of Srs2 is independent of its helicase domain and its Rad51- and PCNA-interaction domains (39–40,50). This suggests that there is a separate Mus81-interaction domain within Srs2. The fact that full-length Srs2 showed lower binding affinity for Mus81 than its N- and C-terminal truncations suggests that the truncated proteins provide better access to a Mus81-interaction domain located within the complex structure of Srs2.

Second, the physical interaction of Srs2 with the Mus81–Mms4 complex results in robust stimulation of its nuclease activity. Kinetic results from the time course experiment shows that the initial reaction rate is linear. Thus, Henri–Michaelis–Menten kinetics could describe the enzymatic activity, in which the linearity of the reaction velocity reflects a role for Srs2 in stabilizing active Mus81–Mms4 on the substrate. Interestingly, neither ATP binding nor its hydrolysis by Srs2 is needed for Srs2 to stimulate nuclease activity (Supplementary Figure S2). A stimulation of Mus81 activity was reported for yeast and human Rad54 proteins (42,47). However, the mechanisms of stimulation are likely to be different, since the interaction between Srs2 and Mus81 does not require ssDNA, as was the case for the Rad54 interaction (42). This conclusion is further supported by the fact that nuclease stimulation requires a small fragment of Srs2 spanning residues 783–898 that does not bind DNA. However, we cannot exclude the possibility that the ability of Srs2 to bind DNA may play a role in stimulation of Mus81 nuclease activity (Figure 3G), since larger fragments of Srs2 that bind DNA show an even higher level of stimulation. In addition, while Rad54 stimulation seems to be evolutionarily conserved, the Srs2 activation is species-specific due to its inability to stimulate human MUS81–EME1 complex.

Third, Srs2 is able to co-immunoprecipitate Mus81 and it co-localizes with Mus81 in cells after DNA damage. The *in vivo* interaction is also supported by expression profiles of the proteins, which both increase in S phase and peak in G2 (53,54). The shared expression profiles and the DNA damage-induced co-localization of Srs2 and Mus81 suggest that there is coordination and regulation of the interaction. Indeed, Mus81 function in yeast is subject to tight cell cycle-dependent control. During S phase, Mus81–Mms4/Eme1 was shown to have low activity presumably to prevent untimely cleavage of replication forks (55–57) since premature activation of the Cdk1/Cdc5/Mus81 pathway induces deleterious crossovers (55). However, in late G2/M mitotic cells, it becomes activated by phosphorylation and is able to cleave any remaining replication-dependent recombination intermediates (55–57). This mechanism both prevents genome instability during replication and ensures processing of late replication intermediates. This facilitates proper chromosome segregation which is a know function of the human MUS81 complex (58,59). Srs2 is also phosphorylated by Cdk1, and this modification, while not affecting the anti-recombinase activity of Srs2, promotes its pro-recombinational repair and was proposed to target Srs2 to specific DNA structures (60). The idea that Srs2 targets Mus81 to such structures via its interaction domain is supported by our *in vitro* experiments as well as the observation that the Srs2 foci precede the Mus81 foci.

Fourth, the ability of Rad51 to inhibit the nuclease activity of Mus81–Mms4 must be specific given that another ssDNA binding protein (RPA) did not present an obstacle for Mus81–Mms4 cleavage (Figure 5 and data not shown). This inhibition was alleviated by Srs2 and its ability to translocate on ssDNA and remove Rad51 (8,9). This conclusion is supported by the fact that the helicase-dead Srs2 mutant, while being able to stimulate Mus81, was not able to suppress the Rad51 inhibition (Figure 5 and Supplementary Figure S2). This indicates that both activities, Rad51 removal and stimulation of the nuclease, could be required for proper processing by Srs2. Srs2 could remove Rad51 from various structures including a displaced extended strand to promote strand annealing, and stimulates the resolution of structures that can be cleaved by Mus81–Mms4 (Figure 8). Indeed, a Rad51-independent activity of Srs2 was previously shown to promote SDSA, as a truncation mutant of Srs2, incapable of binding Rad51, reduced the non-crossover rates, albeit to a lesser extent than an *SRS2* null mutant (61). In addition, DSB repair in a system that monitors *RAD51*-independent events (i.e. break-induced replication (BIR) and single-strand annealing (SSA)) showed a requirement for Srs2 to remove Rad51 from DNA in order to allow downstream repair events (10).

Fifth, we found that Mus81 prevents Srs2 from unwinding recombination/replication intermediates. This observation suggests that Srs2 and Mus81 might coordinate their activities to control the unwinding of specific intermediates in order to stabilize substrates that can be resolved by Mus81–Mms4. We note that the inhibition of unwinding could arise from the sequestering of substrate DNA by Mus81. However, another Srs2- and DNA-binding protein, Mre11, did not affect the helicase activity of Srs2, indicating that the inhibition of Srs2 by Mus81–Mms4 is likely to be specific.

Based on available data we propose a model for the role of Srs2 and Mus81 in processing recombination intermediates (Figure 8). Previous studies have shown that the anti-recombinase activity of Srs2 is responsible for channeling lesions into the post-replication repair pathway by removing Rad51 protein from ssDNA (8–9,62). However, Srs2 also demonstrates pro-recombination activity (11,63). For example, a role of Srs2 in promoting SDSA is supported by the fact that depletion of Srs2 not only reduced DSB

Downloaded from http://nar.oxfordjournals.org/ at Danmarks NaturOG on May 2, 2016

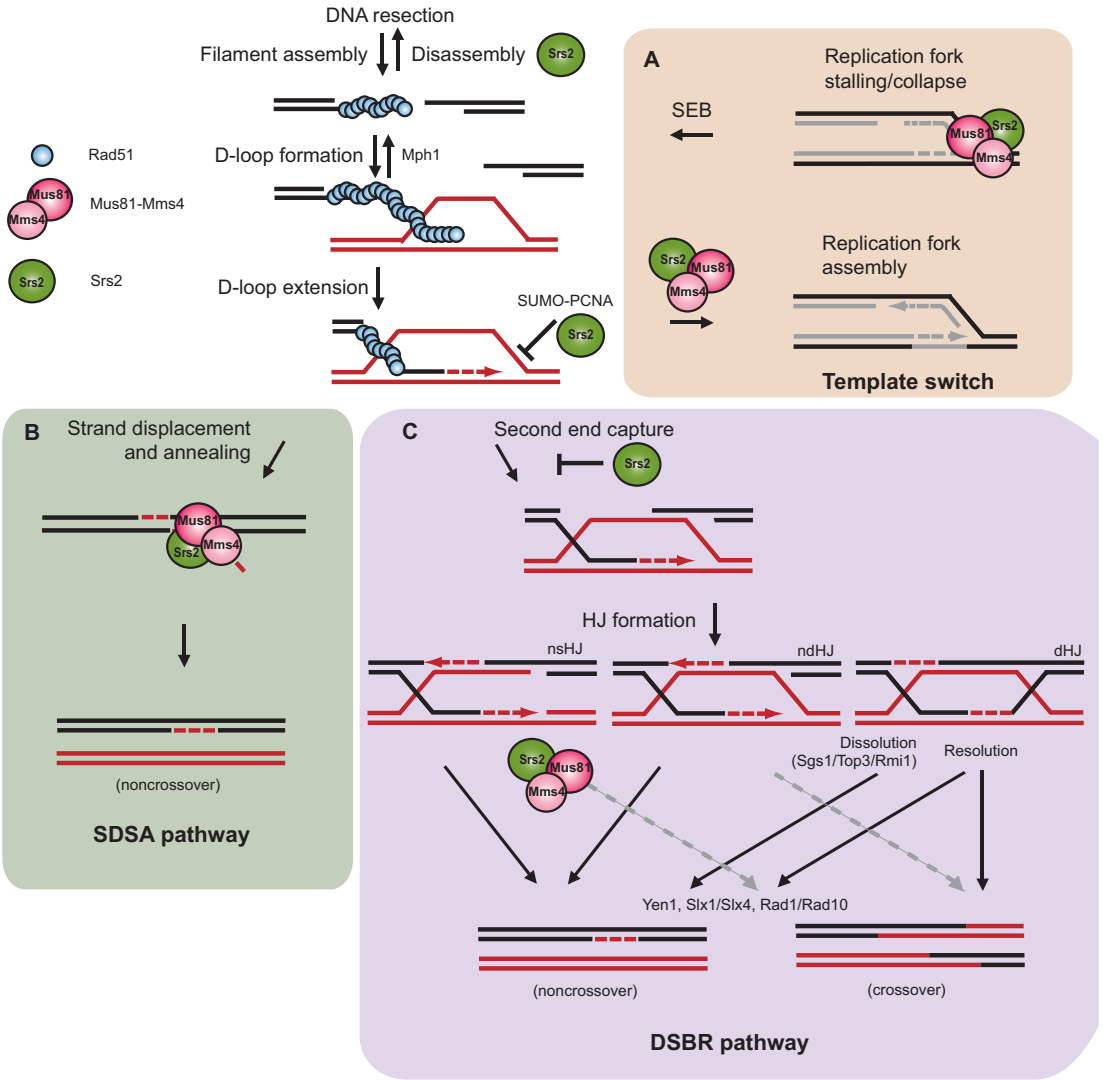

Figure 8. Model for Srs2 and Mus81–Mms4 in resolution of replication and recombination intermediates. Rad51 filament formation is promoted by recombination mediators or disassembled by the action of Srs2. A stable Rad51 filament is able to search for a region of homology that results in the formation of a D-loop structure. (**A**) The D-loop can be unwound by the action of Mph1 helicase or serve as a point for DNA repair extension. The D-loop can alternatively be converted into a replication fork by the coordinated action of Srs2 plus Mus81–Mms4. Similarly Srs2 and Mus81–Mms4 can process stalled replication forks leading to single ended breaks (SEB) that would require HR for repair. (**B**) Coordination between Srs2 and Mus81–Mms4 would also be required to remove Rad51 from various structures including displaced extended strand to promote strand annealing and resolution of structures that can further be cleaved by Mus81–Mms4. (**C**) In classical DSBR pathways Srs2 limits the second-end capture by regulating the length of the extension in a SUMO-PCNA-dependent manner. The indicated subset of structures (nicked single or double Holliday junctions, nsHJ or ndHJ) can alternatively be cleaved by Mus81–Mms4/Srs2 to ensure genomic stability.

repair efficiency and non-crossover events, but it also resulted in a proportional increase in crossovers (10–11,64–65). Based on Srs2's biochemical activities, it was suggested that Srs2 could promote SDSA by preventing second-end capture (10) or by regulating strand elongation within a D-loop structure (12). It was also shown that Srs2 could unwind the invading strand from the template DNA in an oligo-based substrate (66). However, in the context of a Rad51-catalyzed D-loop and following extension of the invading strand, Srs2 is not able to displace the invading or extended strand as efficiently as Mph1 (67,68). A recent study by Mitchel *et al.*, that was able to more specifically distinguish between HJ cleavage, dHJ dissolution and SDSA, demonstrated that while the absence of Srs2 had no effect on crossovers, it resulted in decreased gap-repair efficiencies together with early-appearing non-crossover events (61). They proposed that Srs2 acts on D-loops, and nicked single or double HJs. Shared genetic interactions in both *S. cerevisiae* and *Schizosaccharomyces pombe* indicate that Srs2 and Mus81 function in the same sub-pathway, but it was not clear until now how the anti-recombinase activity of Srs2 could collaborate with Mus81 nuclease activity (18–19,46). Our data provide evidence for the targeting of Mus81 by Srs2 and for coordination of their activities in the processing of various replication/recombination intermediates (Figure 8). This is in line with the ability of Srs2 to recognize

Downloaded from http://nar.oxfordjournals.org/ at Danmarks NaturOG on May 2, 2016

a variety of branched DNA substrates containing a nick that are also favorable substrates for Mus81–Mms4 cleavage (27,32,41–42). Finally, a small deletion within Srs2, corresponding to the Mus81 interaction domain identified here, was previously shown to be almost as detrimental to SDSA as an *srs2* deletion (69). This suggests that the region defined by aa 783–860 of Srs2 is required for SDSA-mediated noncrossovers. However, we note that in our hands this specific deletion mutant is unstable and deficient not only for stimulation of Mus81/Mms4 nuclease but also helicase activity. Mus81/Srs2 activity within the SDSA pathway might also be required when, as a result of over-synthesis, the invading strand is excessively long to a degree where, after displacement and annealing, 3′-flap DNA structures are formed (Figure 8B). Alternatively, similar requirements for processing might be needed for replication restart or when structures arise by annealing of strands with limited homology (Figure 8A).

The hypersensitivity of both Srs2 and Mus81 to CPT suggests possible roles in the repair of DSBs as a consequence of collapsed replication forks at strand nicks. This is distinct from normal PRR since mutants in the PRR pathway are not CPT sensitive (70–73). The interaction of Srs2 with SUMO-PCNA is a prerequisite for recruitment to replication forks (39,74–76), which places Srs2 in a temporal and spatial position to mediate later steps in the repair (Figure 8A). In the case of fission yeast, Srs2 has been reported to promote both fork restart and template exchange at arrested forks (77,78). It has been proposed that this pathway proceeds via a strand invasion/template switch mechanism that uses an intact chromosome arm and generates a D-loop that can be converted into a replisome (Figure 8A). Thus, the coordinated activities of Srs2 and the Mus81 complex might be required not only to process D-loops into replication forks, as proposed for Mus81 fork restart (79), but to cleave stalled forks as reported for yeast and human Mus81 (22–23,31,80).

The notion that Srs2 and Mus81 have additional roles that lie in separate pathways is obvious from the synergistic increase in the DNA damage sensitivity of *mus81 srs2* double mutants compared to single mutants (Figure 6). A similar synergistic increase in CPT sensitivity was observed in fission yeast (46). This is in line with other genetic results showing only partial rescue of the *mus81 sgs1* double mutant by deletion of *RAD51* compared to the more complete rescue of the *srs2 sgs1* strain (18). The increase in Mus81 foci observed in *srs2* strains may reflect not only the formation of toxic recombination intermediates that require Mus81, but also a redundancy in targeting Mus81 to the sites of DNA damage. Such a possibility is reminiscent of Rad54 and BLM which were shown to stimulate and target Mus81 activity (42,47,81). Interestingly, the *srs2-K41R* mutant sensitizes the *mus81* strain to DNA damage even more than *srs2Δ*. This suggests that the inability to remove Rad51 and/or unwind deleterious intermediates is more toxic for the cell than complete loss of Srs2 protein. Additional work will be required to determine if this is caused by a nonfunctional Srs2 protein blocking the processing of recombination intermediates by enzymes such as Mus81.

Our data are also supported by the recent observation that human FBH1 cooperates with MUS81 to promote endonucleolytic DNA cleavage following prolonged replication stress. This suggests that FBH1 helicase is required for MUS81-dependent resolution of toxic intermediates (82). The fact that FBH1 suppresses specific recombination defects in the *srs2* mutant (83) indicates that FBH1 is a functional human homolog of Srs2 and suggests that the mechanism of cooperation with Mus81 is conserved. It is tempting to speculate that various translocases might recruit Mus81 to corresponding intermediates that need to be processed. As stated above, human and yeast RAD54 as well as BLM have been reported to stimulate MUS81 activities (42,47,81). However, Srs2 was not able to stimulate human MUS81–EME1 indicating that this stimulation is species-specific. Additional studies are required to determine which of the Srs2 orthologues might possess this activity in human cells.

In summary, our data help explain the roles of Srs2 and Mus81 in the resolution of recombination/replication intermediates. The uncoordinated regulation of these proteins may lead to aberrant processing of recombination/replication intermediates and contribute to the chromosome instability associated with tumor cells (84). This makes helicases and nucleases promising targets for pharmacologic intervention in cancer therapy.

SUPPLEMENTARY DATA

Supplementary Data are available at NAR Online.

ACKNOWLEDGEMENTS

We would like to thank H. Klein for providing us yeast strains and the members of our laboratories for comments and helpful discussions.

FUNDING

Czech Science Foundation [GACR13-26629S, GACR207/12/2323]; European Regional Development Fund – (Project FNUSA-ICRC) [No. CZ.1.05/1.1.00/02.0123]; The Danish Agency for Science, Technology and Innovation (DFF); Villum Kann Rasmussen Foundation; European Research Council (ERC; to M.L.); NIH [R01GM101613 to S.J.B.].
Conflict of interest statement. None declared.

REFERENCES

1. Sung,P. and Klein,H. (2006) Mechanism of homologous recombination: mediators and helicases take on regulatory functions. *Nat. Rev. Mol. Cell Biol.*, **7**, 739–750.
2. Krejci,L., Altmannova,V., Spirek,M. and Zhao,X. (2012) Homologous recombination and its regulation. *Nucleic Acids Res.*, **40**, 5795–5818.
3. Krogh,B.O. and Symington,L.S. (2004) Recombination proteins in yeast. *Ann. Rev. Genet.*, **38**, 233–271.
4. Marini,V. and Krejci,L. (2010) Srs2: the 'Odd-Job Man' in DNA repair. *DNA Repair*, **9**, 268–275.
5. Rong,L. and Klein,H.L. (1993) Purification and characterization of the SRS2 DNA helicase of the yeast Saccharomyces cerevisiae. *J. Biol. Chem.*, **268**, 1252–1259.
6. Van Komen,S., Macris,M., Sehorn,M.G. and Sung,P. (2006) Purification and assays of Saccharomyces cerevisiae homologous recombination proteins. *Methods Enzymol.*, **408**, 445–463.

Downloaded from http://nar.oxfordjournals.org/ at Danmarks NaturOG on May 2, 2016

7. Aboussekhra,A., Chanet,R., Zgaga,Z., Cassier-Chauvat,C., Heude,M. and Fabre,F. (1989) RADH, a gene of Saccharomyces cerevisiae encoding a putative DNA helicase involved in DNA repair. Characteristics of radH mutants and sequence of the gene. *Nucleic Acids Res.*, **17**, 7211–7219.
8. Krejci,L., Van Komen,S., Li,Y., Villemain,J., Reddy,M.S., Klein,H., Ellenberger,T. and Sung,P. (2003) DNA helicase Srs2 disrupts the Rad51 presynaptic filament. *Nature*, **423**, 305–309.
9. Veaute,X., Jeusset,J., Soustelle,C., Kowalczykowski,S.C., Le Cam,E. and Fabre,F. (2003) The Srs2 helicase prevents recombination by disrupting Rad51 nucleoprotein filaments. *Nature*, **423**, 309–312.
10. Ira,G., Malkova,A., Liberi,G., Foiani,M. and Haber,J.E. (2003) Srs2 and Sgs1-Top3 suppress crossovers during double-strand break repair in yeast. *Cell*, **115**, 401–411.
11. Aylon,Y., Liefshitz,B., Bitan-Banin,G. and Kupiec,M. (2003) Molecular dissection of mitotic recombination in the yeast Saccharomyces cerevisiae. *Mol. Cell. Biol.*, **23**, 1403–1417.
12. Burkovics,P., Sebesta,M., Sisakova,A., Plault,N., Szukacsov,V., Robert,T., Pinter,L., Marini,V., Kolesar,P., Haracska,L. *et al.* (2013) Srs2 mediates PCNA-SUMO-dependent inhibition of DNA repair synthesis. *EMBO J.*, **32**, 742–755.
13. Broomfield,S. and Xiao,W. (2002) Suppression of genetic defects within the RAD6 pathway by srs2 is specific for error-free post-replication repair but not for damage-induced mutagenesis. *Nucleic Acids Res.*, **30**, 732–739.
14. Smirnova,M. and Klein,H.L. (2003) Role of the error-free damage bypass postreplication repair pathway in the maintenance of genomic stability. *Mutat. Res.*, **532**, 117–135.
15. Ulrich,H.D. (2001) The srs2 suppressor of UV sensitivity acts specifically on the RAD5- and MMS2-dependent branch of the RAD6 pathway. *Nucleic Acids Res.*, **29**, 3487–3494.
16. Liberi,G., Chiolo,I., Pellicioli,A., Lopes,M., Plevani,P., Muzi-Falconi,M. and Foiani,M. (2000) Srs2 DNA helicase is involved in checkpoint response and its regulation requires a functional Mec1-dependent pathway and Cdk1 activity. *EMBO J.*, **19**, 5027–5038.
17. Vaze,M.B., Pellicioli,A., Lee,S.E., Ira,G., Liberi,G., Arbel-Eden,A., Foiani,M. and Haber,J.E. (2002) Recovery from checkpoint-mediated arrest after repair of a double-strand break requires Srs2 helicase. *Mol. Cell*, **10**, 373–385.
18. Fabre,F., Chan,A., Heyer,W.D. and Gangloff,S. (2002) Alternate pathways involving Sgs1/Top3, Mus81/ Mms4, and Srs2 prevent formation of toxic recombination intermediates from single-stranded gaps created by DNA replication. *Proc. Natl Acad. Sci. U.S.A.*, **99**, 16887–16892.
19. Gangloff,S., Soustelle,C. and Fabre,F. (2000) Homologous recombination is responsible for cell death in the absence of the Sgs1 and Srs2 helicases. *Nat. Genet.*, **25**, 192–194.
20. Klein,H.L. (2001) Mutations in recombinational repair and in checkpoint control genes suppress the lethal combination of srs2Delta with other DNA repair genes in Saccharomyces cerevisiae. *Genetics*, **157**, 557–565.
21. Lee,S.K., Johnson,R.E., Yu,S.L., Prakash,L. and Prakash,S. (1999) Requirement of yeast SGS1 and SRS2 genes for replication and transcription. *Science*, **286**, 2339–2342.
22. Hanada,K., Budzowska,M., Davies,S.L., van Drunen,E., Onizawa,H., Beverloo,H.B., Maas,A., Essers,J., Hickson,I.D. and Kanaar,R. (2007) The structure-specific endonuclease Mus81 contributes to replication restart by generating double-strand DNA breaks. *Nat. Struct. Mol. Biol.*, **14**, 1096–1104.
23. Hollingsworth,N.M. and Brill,S.J. (2004) The Mus81 solution to resolution: generating meiotic crossovers without Holliday junctions. *Genes Dev.*, **18**, 117–125.
24. Kaliraman,V., Mullen,J.R., Fricke,W.M., Bastin-Shanower,S.A. and Brill,S.J. (2001) Functional overlap between Sgs1-Top3 and the Mms4-Mus81 endonuclease. *Genes Dev.*, **15**, 2730–2740.
25. Whitby,M.C., Osman,F. and Dixon,J. (2003) Cleavage of model replication forks by fission yeast Mus81-Eme1 and budding yeast Mus81-Mms4. *J. Biol. Chem.*, **278**, 6928–6935.
26. Fricke,W.M., Bastin-Shanower,S.A. and Brill,S.J. (2005) Substrate specificity of the Saccharomyces cerevisiae Mus81-Mms4 endonuclease. *DNA Repair*, **4**, 243–251.
27. Ehmsen,K.T. and Heyer,W.D. (2008) Saccharomyces cerevisiae Mus81-Mms4 is a catalytic, DNA structure-selective endonuclease. *Nucleic Acids Res.*, **36**, 2182–2195.
28. Haber,J.E. and Heyer,W.D. (2001) The fuss about Mus81. *Cell*, **107**, 551–554.
29. Interthal,H. and Heyer,W.D. (2000) MUS81 encodes a novel helix-hairpin-helix protein involved in the response to UV- and methylation-induced DNA damage in Saccharomyces cerevisiae. *Mol. Gen. Genet.*, **263**, 812–827.
30. Boddy,M.N., Gaillard,P.H., McDonald,W.H., Shanahan,P., Yates,J.R. III and Russell,P. (2001) Mus81-Eme1 are essential components of a Holliday junction resolvase. *Cell*, **107**, 537–548.
31. Doe,C.L., Ahn,J.S., Dixon,J. and Whitby,M.C. (2002) Mus81-Eme1 and Rqh1 involvement in processing stalled and collapsed replication forks. *J. Biol. Chem.*, **277**, 32753–32759.
32. Bastin-Shanower,S.A., Fricke,W.M., Mullen,J.R. and Brill,S.J. (2003) The mechanism of Mus81-Mms4 cleavage site selection distinguishes it from the homologous endonuclease Rad1-Rad10. *Mol. Cell. Biol.*, **23**, 3487–3496.
33. de los Santos,T., Hunter,N., Lee,C., Larkin,B., Loidl,J. and Hollingsworth,N.M. (2003) The Mus81/Mms4 endonuclease acts independently of double-Holliday junction resolution to promote a distinct subset of crossovers during meiosis in budding yeast. *Genetics*, **164**, 81–94.
34. Mullen,J.R., Kaliraman,V., Ibrahim,S.S. and Brill,S.J. (2001) Requirement for three novel protein complexes in the absence of the Sgs1 DNA helicase in Saccharomyces cerevisiae. *Genetics*, **157**, 103–118.
35. Sherman,F., Fink,G. R. and Hicks,J. B. (1983) *Methods in Yeast Genetics: Laboratory Manual*. Cold Spring Harbor, NY.
36. Sherman,F. (1991) Getting started with yeast. *Methods Enzymol.*, **194**, 3–21.
37. Zhao,X., Muller,E.G. and Rothstein,R. (1998) A suppressor of two essential checkpoint genes identifies a novel protein that negatively affects dNTP pools. *Mol. Cell*, **2**, 329–340.
38. Thomas,B.J. and Rothstein,R. (1989) Elevated recombination rates in transcriptionally active DNA. *Cell*, **56**, 619–630.
39. Kolesar,P., Sarangi,P., Altmannova,V., Zhao,X. and Krejci,L. (2012) Dual roles of the SUMO-interacting motif in the regulation of Srs2 sumoylation. *Nucleic Acids Res.*, **40**, 7831–7843.
40. Colavito,S., Macris-Kiss,M., Seong,C., Gleeson,O., Greene,E.C., Klein,H.L., Krejci,L. and Sung,P. (2009) Functional significance of the Rad51-Srs2 complex in Rad51 presynaptic filament disruption. *Nucleic Acids Res.*, **37**, 6754–6764.
41. Marini,V. and Krejci,L. (2012) Unwinding of synthetic replication and recombination substrates by Srs2. *DNA Repair*, **11**, 789–798.
42. Matulova,P., Marini,V., Burgess,R.C., Sisakova,A., Kwon,Y., Rothstein,R., Sung,P. and Krejci,L. (2009) Cooperativity of Mus81.Mms4 with Rad54 in the resolution of recombination and replication intermediates. *J. Biol. Chem.*, **284**, 7733–7745.
43. Trujillo,K.M. and Sung,P. (2001) DNA structure-specific nuclease activities in the Saccharomyces cerevisiae Rad50*Mre11 complex. *J. Biol. Chem.*, **276**, 35458–35464.
44. Krejci,L., Damborsky,J., Thomsen,B., Duno,M. and Bendixen,C. (2001) Molecular dissection of interactions between Rad51 and members of the recombination-repair group. *Mol. Cell. Biol.*, **21**, 966–976.
45. Eckert-Boulet,N., Rothstein,R. and Lisby,M. (2011) Cell biology of homologous recombination in yeast. *Methods Mol. Biol.*, **745**, 523–536.
46. Doe,C.L. and Whitby,M.C. (2004) The involvement of Srs2 in post-replication repair and homologous recombination in fission yeast. *Nucleic Acids Res.*, **32**, 1480–1491.
47. Mazina,O.M. and Mazin,A.V. (2008) Human Rad54 protein stimulates human Mus81-Eme1 endonuclease. *Proc. Natl Acad. Sci. U.S.A.*, **105**, 18249–18254.
48. Kang,M.J., Lee,C.H., Kang,Y.H., Cho,I.T., Nguyen,T.A. and Seo,Y.S. (2010) Genetic and functional interactions between Mus81-Mms4 and Rad27. *Nucleic Acids Res.*, **38**, 7611–7625.
49. Van Komen,S., Reddy,M.S., Krejci,L., Klein,H. and Sung,P. (2003) ATPase and DNA helicase activities of the Saccharomyces cerevisiae anti-recombinase Srs2. *J. Biol. Chem.*, **278**, 44331–44337.
50. Krejci,L., Macris,M., Li,Y., Van Komen,S., Villemain,J., Ellenberger,T., Klein,H. and Sung,P. (2004) Role of ATP hydrolysis

Downloaded from http://nar.oxfordjournals.org/ at Danmarks NaturOG on May 2, 2016

in the antirecombinase function of Saccharomyces cerevisiae Srs2 protein. *J. Biol. Chem.*, **279**, 23193–23199.
51. Ciccia,A., McDonald,N. and West,S.C. (2008) Structural and functional relationships of the XPF/MUS81 family of proteins. *Annu. Rev. Biochem.*, **77**, 259–287.
52. Munoz-Galvan,S., Tous,C., Blanco,M.G., Schwartz,E.K., Ehmsen,K.T., West,S.C., Heyer,W.D. and Aguilera,A. (2012) Distinct roles of Mus81, Yen1, Slx1-Slx4, and Rad1 nucleases in the repair of replication-born double-strand breaks by sister chromatid exchange. *Mol. Cell. Biol.*, **32**, 1592–1603.
53. Heude,M., Chanet,R. and Fabre,F. (1995) Regulation of the Saccharomyces cerevisiae Srs2 helicase during the mitotic cell cycle, meiosis and after irradiation. *Mol. Gen. Genet.*, **248**, 59–68.
54. Gao,H., Chen,X.B. and McGowan,C.H. (2003) Mus81 endonuclease localizes to nucleoli and to regions of DNA damage in human S-phase cells. *Mol. Biol. Cell*, **14**, 4826–4834.
55. Szakal,B. and Branzei,D. (2013) Premature Cdk1/Cdc5/Mus81 pathway activation induces aberrant replication and deleterious crossover. *EMBO J.*, **32**, 1155–1167.
56. Gallo-Fernandez,M., Saugar,I., Ortiz-Bazan,M.A., Vazquez,M.V. and Tercero,J.A. (2012) Cell cycle-dependent regulation of the nuclease activity of Mus81-Eme1/Mms4. *Nucleic Acids Res.*, **40**, 8325–8335.
57. Matos,J., Blanco,M.G., Maslen,S., Skehel,J.M. and West,S.C. (2011) Regulatory control of the resolution of DNA recombination intermediates during meiosis and mitosis. *Cell*, **147**, 158–172.
58. Naim,V., Wilhelm,T., Debatisse,M. and Rosselli,F. (2013) ERCC1 and MUS81-EME1 promote sister chromatid separation by processing late replication intermediates at common fragile sites during mitosis. *Nat. Cell Biol.*, **15**, 1008–1015.
59. Ying,S., Minocherhomji,S., Chan,K.L., Palmai-Pallag,T., Chu,W.K., Wass,T., Mankouri,H.W., Liu,Y. and Hickson,I.D. (2013) MUS81 promotes common fragile site expression. *Nat. Cell Biol.*, **15**, 1001–1007.
60. Saponaro,M., Callahan,D., Zheng,X., Krejci,L., Haber,J.E., Klein,H.L. and Liberi,G. (2010) Cdk1 targets Srs2 to complete synthesis-dependent strand annealing and to promote recombinational repair. *PLoS Genet.*, **6**, e1000858.
61. Mitchel,K., Lehner,K. and Jinks-Robertson,S. (2013) Heteroduplex DNA position defines the roles of the Sgs1, Srs2, and Mph1 helicases in promoting distinct recombination outcomes. *PLoS Genet.*, **9**, e1003340.
62. Chanet,R., Heude,M., Adjiri,A., Maloisel,L. and Fabre,F. (1996) Semidominant mutations in the yeast Rad51 protein and their relationships with the Srs2 helicase. *Mol. Cell. Biol.*, **16**, 4782–4789.
63. Friedl,A.A., Liefshitz,B., Steinlauf,R. and Kupiec,M. (2001) Deletion of the SRS2 gene suppresses elevated recombination and DNA damage sensitivity in rad5 and rad18 mutants of Saccharomyces cerevisiae. *Mutat. Res.*, **486**, 137–146.
64. Welz-Voegele,C. and Jinks-Robertson,S. (2008) Sequence divergence impedes crossover more than noncrossover events during mitotic gap repair in yeast. *Genetics*, **179**, 1251–1262.
65. Robert,T., Dervins,D., Fabre,F. and Gangloff,S. (2006) Mrc1 and Srs2 are major actors in the regulation of spontaneous crossover. *EMBO J.*, **25**, 2837–2846.
66. Dupaigne,P., Le Breton,C., Fabre,F., Gangloff,S., Le Cam,E. and Veaute,X. (2008) The Srs2 helicase activity is stimulated by Rad51 filaments on dsDNA: implications for crossover incidence during mitotic recombination. *Mol. Cell*, **29**, 243–254.
67. Prakash,R., Satory,D., Dray,E., Papusha,A., Scheller,J., Kramer,W., Krejci,L., Klein,H., Haber,J.E., Sung,P. *et al.* (2009) Yeast Mph1 helicase dissociates Rad51-made D-loops: implications for crossover control in mitotic recombination. *Genes Dev.*, **23**, 67–79.
68. Sebesta,M., Burkovics,P., Haracska,L. and Krejci,L. (2011) Reconstitution of DNA repair synthesis in vitro and the role of polymerase and helicase activities. *DNA Repair*, **10**, 567–576.
69. Miura,T., Shibata,T. and Kusano,K. (2013) Putative antirecombinase Srs2 DNA helicase promotes noncrossover homologous recombination avoiding loss of heterozygosity. *Proc. Natl Acad. Sci. U.S.A.*, **110**, 16067–16072.
70. Valencia-Burton,M., Oki,M., Johnson,J., Seier,T.A., Kamakaka,R. and Haber,J.E. (2006) Different mating-type-regulated genes affect the DNA repair defects of Saccharomyces RAD51, RAD52 and RAD55 mutants. *Genetics*, **174**, 41–55.
71. Verkade,H.M., Teli,T., Laursen,L.V., Murray,J.M. and O'Connell,M.J. (2001) A homologue of the Rad18 postreplication repair gene is required for DNA damage responses throughout the fission yeast cell cycle. *Mol. Genet. Genomics*, **265**, 993–1003.
72. Doe,C.L., Murray,J.M., Shayeghi,M., Hoskins,M., Lehmann,A.R., Carr,A.M. and Watts,F.Z. (1993) Cloning and characterisation of the Schizosaccharomyces pombe rad8 gene, a member of the SNF2 helicase family. *Nucleic Acids Res.*, **21**, 5964–5971.
73. Simon,J.A., Szankasi,P., Nguyen,D.K., Ludlow,C., Dunstan,H.M., Roberts,C.J., Jensen,E.L., Hartwell,L.H. and Friend,S.H. (2000) Differential toxicities of anticancer agents among DNA repair and checkpoint mutants of Saccharomyces cerevisiae. *Cancer Res.*, **60**, 328–333.
74. Papouli,E., Chen,S., Davies,A.A., Huttner,D., Krejci,L., Sung,P. and Ulrich,H.D. (2005) Crosstalk between SUMO and ubiquitin on PCNA is mediated by recruitment of the helicase Srs2p. *Mol. Cell*, **19**, 123–133.
75. Pfander,B., Moldovan,G.L., Sacher,M., Hoege,C. and Jentsch,S. (2005) SUMO-modified PCNA recruits Srs2 to prevent recombination during S phase. *Nature*, **436**, 428–433.
76. Burgess,R.C., Lisby,M., Altmannova,V., Krejci,L., Sung,P. and Rothstein,R. (2009) Localization of recombination proteins and Srs2 reveals anti-recombinase function in vivo. *J. Cell Biol.*, **185**, 969–981.
77. Inagawa,T., Yamada-Inagawa,T., Eydmann,T., Mian,I.S., Wang,T.S. and Dalgaard,J.Z. (2009) Schizosaccharomyces pombe Rtf2 mediates site-specific replication termination by inhibiting replication restart. *Proc. Natl Acad. Sci. U.S.A.*, **106**, 7927–7932.
78. Lambert,S., Mizuno,K., Blaisonneau,J., Martineau,S., Chanet,R., Freon,K., Murray,J.M., Carr,A.M. and Baldacci,G. (2010) Homologous recombination restarts blocked replication forks at the expense of genome rearrangements by template exchange. *Mol. Cell*, **39**, 346–359.
79. Roseaulin,L., Yamada,Y., Tsutsui,Y., Russell,P., Iwasaki,H. and Arcangioli,B. (2008) Mus81 is essential for sister chromatid recombination at broken replication forks. *EMBO J.*, **27**, 1378–1387.
80. Froget,B., Blaisonneau,J., Lambert,S. and Baldacci,G. (2008) Cleavage of stalled forks by fission yeast Mus81/Eme1 in absence of DNA replication checkpoint. *Mol. Biol. Cell*, **19**, 445–456.
81. Zhang,R., Sengupta,S., Yang,Q., Linke,S.P., Yanaihara,N., Bradsher,J., Blais,V., McGowan,C.H. and Harris,C.C. (2005) BLM helicase facilitates Mus81 endonuclease activity in human cells. *Cancer Res.*, **65**, 2526–2531.
82. Fugger,K., Chu,W.K., Haahr,P., Kousholt,A.N., Beck,H., Payne,M.J., Hanada,K., Hickson,I.D. and Sorensen,C.S. (2013) FBH1 co-operates with MUS81 in inducing DNA double-strand breaks and cell death following replication stress. *Nat. Commun.*, **4**, 1423.
83. Chiolo,I., Saponaro,M., Baryshnikova,A., Kim,J.H., Seo,Y.S. and Liberi,G. (2007) The human F-Box DNA helicase FBH1 faces Saccharomyces cerevisiae Srs2 and postreplication repair pathway roles. *Mol. Cell. Biol.*, **27**, 7439–7450.
84. Schvartzman,J.M., Sotillo,R. and Benezra,R. (2010) Mitotic chromosomal instability and cancer: mouse modelling of the human disease. *Nat. Rev. Cancer*, **10**, 102–115.

Downloaded from http://nar.oxfordjournals.org/ at Danmarks NaturOG on May 2, 2016